

**ISTANBUL TECHNICAL UNIVERSITY ★ INFORMATICS INSTITUTE**

**HYPERSPECTRAL IMAGE  
COMPRESSION USING SPARSE REPRESENTATIONS  
AND WAVELET TRANSFORM BASED SPECTRAL DECORRELATION**

**M.Sc. THESIS**

**Hayder JAWDHARI**

**Department of Applied Informatics**

**Applied Informatics Programme**

**JUNE 2017**



**HYPERSPECTRAL IMAGE  
COMPRESSION USING SPARSE REPRESENTATIONS  
AND WAVELET TRANSFORM BASED SPECTRAL DECORRELATION**

**M.Sc. THESIS**

**Hayder Jawdhari  
708151020**

**Department of Applied Informatics**

**Applied Informatics Programme**

**Thesis Advisor: Assoc.Prof.Dr. Behçet Uğur Töreyn**

**JUNE 2017**



**İSTANBUL TEKNİK ÜNİVERSİTESİ ★ BİLİŞİM ENSTİTÜSÜ**

**SEYREK GÖSTERİMLER VE DALGACIK DÖNÜŞÜMÜNE  
DAYALI İZGEL İLİNTİSİZLEŞTİRME KULLANARAK  
HİPERSPEKTRAL GÖRÜNTÜ SIKIŞTIRMA**

**YÜKSEK LİSANS TEZİ**

**Hayder Jawdhari  
708151020**

**Bilişim Enstitüsü  
Bilişim Uygulamaları Programı**

**Tez Danışmanı: Doç.Dr. Behçet Uğur Töreyin**

**Haziran 2017**



Hayder-Jawdhari, A M.Sc. student of ITU Informatics Institute student ID 708151020, successfully defended the thesis/dissertation entitled Hyperspectral Image Compression Using Sparse Representations and Wavelet Transform based Spectral Decorrelation, ” which he prepared after fulfilling the requirements specified in the associated legislations, before the jury whose signatures are below.

**Thesis Advisor :** **Doç.Dr. Behçet Uğur TÖREYİN**  
İstanbul Technical University



**Jury Members :** **Prof. Dr. Lütfiye DURAK ATA**  
İstanbul Technical University



**Yard. Doç. Dr. Alp ERTÜRK**  
Kocaeli University



**Date of Submission : 4 May 2017**

**Date of Defense : 6 June 2017**





## **My Parent**

To my angel in life, the meaning of love and the meaning of compassion and dedication, the secret of my smile in life ,all the world's words are not enough to describe thanks to your character living your life for us, you gave me the right way, and I hope that you accept this little.....**My Father.**

The woman who nursed me in my childhood ...She taught me ... and took me with her tenderness ...always .. I find it beside me in my crisis ...To the most precious people, my heart knows her. With all the love I give her ... A word of thanks...

I thank your tears, your anxiety and your prayers every night and every day, I hope that you accept this little..... **My Mother.**

## **My Family**

If I had to give you my eyes to put it in your hands .. If I had to give you my heart to remove it from my chest and presented it to you .. If I had to give you my age, I would have recorded my days in your name. But I have only so many words of sincere expressions. May it be my gift to you with my love, and God will keep the sun of your presence and the warmth of our festivals.....**My Spouse.**

My children.. **NOOR and ABDUSATTAR**

My brothers especially my sister (**Mariam**).

**Hayder Jawdhari**



## **FOREWORD**

I would like to thank my advisor Doç.Dr. Behçet Uğur Töreyn for his support and valuable guidance. Despite all the words of thanks considered low for the expression of a man carrying noble message, the mind of the lead and finally yet importantly, the heart expresses the beautiful original.

May 2017

Hayder Jawdhari



## TABLE OF CONTENTS

	<u>Page</u>
<b>FOREWORD</b> .....	<b>ix</b>
<b>TABLE OF CONTENTS</b> .....	<b>xi</b>
<b>ABBREVIATIONS</b> .....	<b>xiii</b>
<b>LIST OF TABLES</b> .....	<b>xv</b>
<b>LIST OF FIGURES</b> .....	<b>xvii</b>
<b>SUMMARY</b> .....	<b>xix</b>
<b>ÖZET</b> .....	<b>xxi</b>
<b>1. INTRODUCTION</b> .....	<b>1</b>
1.1 Contribution of the Thesis.....	3
<b>2. LITERATURE REVIEW</b> .....	<b>5</b>
2.1 Lossy compression of hyperspectral images .....	5
2.2 Lossless hyperspectral image compression and decorrelation approaches.....	6
2.3 Lossy and lossless hyperspectral image compression.....	8
2.4 Distributed Source Coding Based Hyperspectral Image Compression.....	9
2.5 dictionary learning for hyperspectral image compression .....	10
2.6 Sparse representation in image processing for hyperspectral data .....	11
<b>3. METHODOLOGY</b> .....	<b>15</b>
3.1 Spectral Decorrelation.....	15
3.2 High subband images are compressed using JPEG2000 codec in lossless mode.	18
3.3 Low subband data block is processed to obtain a sparse representation .....	18
3.3.1 Sparse coding .....	18
3.3.1.1 Least absolute shrinkage and selection operator.....	19
3.3.1.2 Basis pursuit .....	20
3.3.2 Dictionary learning.....	20
3.3.3 Sparse coding and dictionary learning.....	21
<b>4. RESULTS AND DISCUSSIONS</b> .....	<b>27</b>
4.1 Experimental data set.....	27
4.2 Rate-distortion comparison results .....	36
<b>5. CONCLUSIONS AND RECOMMENDATIONS</b> .....	<b>45</b>
<b>REFERENCES</b> .....	<b>47</b>
<b>CURRICULUM VITAE</b> .....	<b>57</b>



## ABBREVIATIONS

<b>1-level</b>	: One- Level
<b>2D</b>	: Two- Dimensions
<b>2-level</b>	: Two- Level
<b>3D</b>	: Three- Dimensions
<b>3-level</b>	: Three - Level
<b>ADMM</b>	: Alternating Direction Method of Multipliers
<b>ADMM</b>	: Alternating Direction Method of Multipliers
<b>AVIRIS</b>	: Airborne Visible / Infrared Imaging Spectrometer
<b>BEZW</b>	: Binary Embedded Zerotree Wavelet
<b>BP</b>	: Basis Pursuit
<b>BPS</b>	: Bit per Sample
<b>CWT</b>	: Continuous Wavelet Transform
<b>DCT</b>	: Discrete Cosine Transform
<b>DSC</b>	: Distributed Source Coding
<b>DWT</b>	: Discrete Wavelet Transform
<b>JEPG2000</b>	: Joint Photographic Experts Group
<b>KLT</b>	: Karhunen–Loève Transform
<b>LASSO</b>	: Least Absolute Shrinkage and Selection Operator
<b>MSE</b>	: Mean Squared Error
<b>NLPCA</b>	: Nonlinear Principal Component Analysis
<b>OMP</b>	: Orthogonal Matching Pursuit
<b>OMP</b>	: Orthogonal Matching Pursuit
<b>PCA</b>	: Principal Component Analysis
<b>PSNR</b>	: Peak Signal to Noise Ratio
<b>PWSR</b>	: PixelWise Sparse Representation
<b>RGB</b>	: Red, Green and Blue
<b>RTDLT</b>	: Reversible Time-Domain Lapped Transform
<b>SAM</b>	: Spectral Angle Mapping
<b>SPIHT</b>	: Set Partitioning In Hierarchical Trees
<b>SR</b>	: Sparse Representation
<b>SROI</b>	: Spatial Region of Interest
<b>ST</b>	: Spatial-Temporal
<b>TROI</b>	: Temporal Region of Interest
<b>VQ</b>	: Vector Quantization
<b>WT</b>	: Wavelet Transform





## LIST OF TABLES

	<u>Page</u>
<b>Table 3.1</b> : High pass filters for Various Integer Wavelet Transforms.....	16
<b>Table 3.2</b> : High pass filters for Various Integer Wavelet Transforms.....	16
<b>Table 4.1</b> : Image specifications of AVIRIS/HYPERION hyperspectral data.....	27
<b>Table 4.2</b> : Haar filter bank, Low Altitude, LASSO sparse representation .....	29
<b>Table 4.3</b> : Haar filter bank, Low Altitude, BP sparse representation .....	29
<b>Table 4.4</b> : $9\setminus 7$ filter bank, Low Altitude, LASSO sparse representation .....	30
<b>Table 4.5</b> : $9\setminus 7$ filter bank, Low Altitude, BP sparse representation .....	30
<b>Table 4.6</b> : $5\setminus 3$ filter bank, Low Altitude, LASSO sparse representation .....	30
<b>Table 4.7</b> : $5\setminus 3$ filter bank, Low Altitude, BP sparse representation .....	30
<b>Table 4.8</b> : $9\setminus 3$ filter bank, Low Altitude, LASSO sparse representation.....	31
<b>Table 4.9</b> : $9\setminus 3$ filter bank, Low Altitude, BP sparse representation .....	31
<b>Table 4.10</b> : $5\setminus 11$ filter bank, Low Altitude, LASSO sparse representation.....	31
<b>Table 4.11</b> : $5\setminus 11$ filter bank, Low Altitude, BP sparse representation.....	31
<b>Table 4.12</b> : $2\setminus 6$ filter bank, Low Altitude, LASSO sparse representation.....	32
<b>Table 4.13</b> : $2\setminus 6$ filter bank, Low Altitude, BP sparse representation.....	32
<b>Table 4.14</b> : Haar filter bank, Erta Ale, LASSO sparse representation .....	32
<b>Table 4.15</b> : Haar filter bank, Erta Ale, BP sparse representation .....	32
<b>Table 4.16</b> : $9\setminus 7$ filter bank, Erta Ale, LASSO sparse representation .....	33
<b>Table 4.17</b> : $9\setminus 7$ filter bank, Erta Ale, BP sparse representation.....	33
<b>Table 4.18</b> : $5\setminus 3$ filter bank, Erta Ale, LASSO sparse representation.....	33
<b>Table 4.19</b> : $5\setminus 3$ filter bank, Erta Ale, BP sparse representation.....	33
<b>Table 4.20</b> : $9\setminus 3$ filter bank, Erta Ale, LASSO sparse representation.....	34
<b>Table 4.21</b> : $9\setminus 3$ filter bank, Erta Ale, BP sparse representation.....	34
<b>Table 4.22</b> : $5\setminus 11$ filter bank, Erta Ale, LASSO sparse representation.....	34
<b>Table 4.23</b> : $5\setminus 11$ filter bank, Erta Ale, BP sparse representation.....	34
<b>Table 4.24</b> : $2\setminus 6$ filter bank, Erta Ale, LASSO sparse representation .....	35
<b>Table 4.25</b> : $2\setminus 6$ filter bank, Erta Ale, BP sparse representation.....	35



## LIST OF FIGURES

	<u>Page</u>
<b>Figure 1.1</b> : A hyperspectral data cube sample (Low Altitude). The data cube is formed by a stack of two dimensional band images where bands make up the spectral component of the data.....	2
<b>Figure 3.1</b> : The hyperspectral data, X, is decomposed into low, XL, and high, XH subband blocks, in the spectral dimension. This is achieved by decomposing $x_{i,j}[k]$ for each line and sample,(i,j) location, into low low-band, $x_{li,j}[k]$ , and high-band, $x_{hi,j}[k]$ , components.....	17
<b>Figure 3.2</b> : Single-level integer wavelet transform. Each $x_{i,j}[k]$ corresponding to the spectral content at location (i,j) is decomposed into two components, namely, $x_{li,j}[k]$ , and $x_{hi,j}[k]$ .....	17
<b>Figure 3.3</b> : Two-level integer wavelet transform applied to $x_{i,j}[k]$ for further spectral decorrelation. In this thesis, upto three levels are applied.....	25
<b>Figure 3.4</b> : Single-level (perfect) reconstruction stage corresponding to integer wavelet transforms .....	25
<b>Figure 4.1</b> : Three-level spectral decorrelation of Hyperspectral data. The data blocks named as H, LH and LLH, are all compressed using JPEG2000 – lossles mode, whereas, LLL and LL are compressed using sparse representations .....	27
<b>Figure 4.2</b> : Performance comparison of online-learning-based hyperspectral image- compression algorithms with lasso and bp sparse representation for Low Altitude and Erta Ale are cropped as 256 lines by 256 samples by 242 bands. Using haar filter bank (a) single level , (b) 2-level, (c) 3-level decommission .....	37
<b>Figure 4.3</b> : Performance comparison of online-learning-based hyperspectral image- compression algorithms with lasso and bp sparse representation for Low Altitude and Erta Ale are cropped as 256 lines by 256 samples by 242 bands. Using 9\7 filter bank (a)single level , (b) 2-level, (c) 3-decommission.....	38
<b>Figure 4.4</b> : Performance comparison of online-learning-based hyperspectral image- compression algorithms with lasso and bp sparse representation for Low Altitude and Erta Ale are cropped as 256 lines by 256 samples by 242 bands. Using 5\3 filter bank (a)single level , (b) 2-level, (c) 3-level decommission .....	39
<b>Figure 4.5</b> : Performance comparison of online-learning-based hyperspectral image- compression algorithms with lasso and bp sparse representation for Low Altitude and Erta Ale are cropped as 256 lines by 256 samples by 242 bands. Using 9\3 filter bank (a)single level , (b) 2-level, (c) 3-level decommission .....	40

**Figure 4.6** : Performance comparison of online-learning-based hyperspectral image- compression algorithms with lasso and bp sparse representation for Low Altitude and Erta Ale are cropped as 256 lines by 256 samples by 242 bands. Using 5\11 filter bank (a) single level , (b) 2-level, (c) 3-level decommission.....41

**Figure 4.7** : Performance comparison of online-learning-based hyperspectral image-compression algorithms with lasso and bp sparse representation for Low Altitude and Erta Ale are cropped as 256 lines by 256 samples by 242 bands. Using 2\6 filter bank (a)single level , (b) 2-level, (c) 3-level decommission.....42

# **HYPERSPECTRAL IMAGE COMPRESSION USING SPARSE REPRESENTATIONS AND WAVELET TRANSFORM BASED SPECTRAL DECORRELATION**

## **SUMMARY**

Being a spectral imaging technique, hyperspectral imagery enables acquisition of electromagnetic spectrum data in hundreds of narrow bands. The chemical composition of objects within the viewing range of hyperspectral sensors may be analyzed with the help hyperspectral imaging techniques. Providing a huge amount of data comes with a heavy cost of size. To that extent, hyperspectral compression methods become essential for transmission and storage purposes.

There are two fundamental ways for data compression, namely, lossless and lossy. Lossy methods aims at compressing the data as much as possible while keeping the reconstructed data quality as high as possible. On the other hand, lossless compression techniques, as the name suggests, are targeted towards compressing the data in a lossless manner with the largest possible compression ratio value defined as the ration of uncompressed data size to the size of the compressed data. Lossless compression schemes typically achieve much higher compression ratios as compared with lossy techniques.

For hyperspectral compression purposes, data-driven approaches, such as dictionary learning based lossy compression methods, yield better compression performance compared with other state-of-the-art methods. Regarding the lossless compression methods for hyperspectral imagery, integer wavelet transform based techniques are reported to perform better in terms of compression ratio.

In this thesis, a novel hyperspectral image compression approach that blends a fully data-driven technique based on sparse representations and an integer wavelet transform based algorithm is proposed. The hyperspectral data is spectrally decorrelated using various integer wavelet filters at different levels. The decorrelated data is then processed according to its frequency content in such a way that highly correlated, sparse high-band block is compressed in a lossless fashion with JPEG2000. On the other hand, a sparse representation is obtained for the low-band block making it possible to represent the lower subband data block using a few number of coefficients.

Experimental results indicate that, the proposed hybrid method perfoms better than the existing hyperspectral image compression techniques.



# SEYREK GÖSTERİMLER VE DALGACIK DÖNÜŞÜMÜNE DAYALI İZGEL İLİNTİSİZLEŞTİRME KULLANARAK HİPERSPEKTRAL GÖRÜNTÜ SIKIŞTIRMA

## ÖZET

Son yıllarda, görüntü işleme alanındaki çalışmaların sayısında ve çeşidinde artış olduğu gözlenmektedir. Birçok dalga boyu bandında algılanan enerji üzerinde hassas kayıt yapabilmek için uzaktan algılama bu alanlardan en önemlisidir. Hipperspektral görüntüler, dijital görüntülerin ve spektroskopinin güçlü yanlarını birleştirir. Bir hiperspektral kamera, komşu spektral bantların büyük bir kısmı için ışık yoğunluğunu yakalar. Hiperspektral görüntüler, farklı izgelere olan duyarlılıklarından ötürü, algıladıkları nesnelerin kimyasal içeriğine ilişkin önemli bilgiler sunmaktadır.

Uydu görüntüleri ve özellikle hiperspektral görüntüler, farklı bilimlerin birçok alanı için önemli veri kaynağıdır. Uydu görüntüleri, insan gözü veya diğer teknolojiler tarafından algılanamayan, yeryüzündeki geniş bir alanı kaplar. Uzaktan algılama terimi ilk olarak 1960'larda kullanıldı. Bu teknoloji, yeryüzünün uzaktan gözlenmesini esas almıştır. Yeryüzünü izlemek için farklı yükseklikteki uydular kullanılır.

Bu çalışmada, çevrimiçi öğrenmeyi temel alan seyrek kodlamayı kullanarak kayıplı bir hiperspektral görüntü sıkıştırma yöntemi önerilmektedir. Hiperspektral görüntüleri çevrimiçi sözlük öğrenme yöntemine dayanan seyrek kodlama algoritması uygulayarak temsil etmek için en az sayıda katsayı elde edilir. Sonuçlar, sıfır olmayan sözlük öğelerinin bir ön analizinin, genel sıkıştırma kalitesini iyileştirmede yardımcı olabileceğini ortaya koymaktadır.

Seyrek kodlama tabanlı hiperspektral görüntü sıkıştırma, literatürdeki tekniğin mevcut durumunu yansıtan yöntemlere göre, özellikle düşük bit hızlarında daha iyi veri hızı-bozunum başarımı vermektedir

Seyrek gösterim, önceden eğitilmiş bir sözlükten birkaç sözcüğün (atomun) doğrusal bileşimi olarak sinyalleri modelleme yeteneğine sahiptir. Sinyallerin gösterilmesinde çok seyrek doğaya neden olan uyarlanabilir bir sözlük öğrenmeyi sağlar. Bu çalışmada, seyrek gösterim, kayıplı bir hiperspektral veri sıkıştırma çerçevesinde konuşlandırılmıştır. Spektral korelasyonun yanı sıra hem spektral hem de mekansal korelasyondan yararlanan sözlükler çevrimiçi sözlük öğrenimi kullanılarak eğitilir. Daha sonra, hiperspektral bir veri, seyrek kodlama yoluyla öğrenilen sözlük kullanılarak gösterilir. Oluşan seyrek katsayılar nihai bit akışı formüle etmek için kodlanır. Bir dizi hiperspektral veri kümesindeki deneysel sonuçlar, önerilen yaklaşımın hız-bozulma performansı açısından 3D-SPIHT gibi dalgacık tabanlı yöntemlerle rekabet ettiğini göstermektedir.

Seyrek modeller, sıfır olmayan elementlerle verilerin temsil edilmesini sağlar. Seyrek modellerin bu özelliği, veri sıkıştırma amacıyla seyrek modellerin kullanılmasının uygun olabileceğini düşündürmektedir.

Teknolojinin gelişmesiyle birlikte, görüntüleme teknolojileri, hiperspektral görüntüleme gibi görüntüleme yeteneklerine ve gelişmiş görüntüleme özelliklerini olanaklı kılmıştır. Hiperspektral görüntülerin kullanılması ile, spektral düzlemdeki dar bant genişlikleri ile çok büyük miktarda veri işlenmeye başlandı ve daha yüksek hesaplama maliyetleri oluştu. Sınıflandırma performanslarındaki artışa rağmen, bu büyük boyutlu verilerin boyutunun azaltılması önemli bir olgu hâline geldi.

Bu çalışmada, çevrimiçi öğrenmeyi kullanan seyrekliğe dayalı hiperspektral görüntü sıkıştırma yöntemleri için bir çerçeve ve dalgacık dönüşümüne dayalı bir izgel ilintisizleştirme önerilmektedir. Bu amaçla, tamsayı katsayılı dalgacık dönüşümü süzgeçleriyle izgel ilintisizleştirilen hiperspektral veri, JPEG2000 kodeği ile kayıpsız olarak, seyrek gösterimlere dayalı yöntemle ise kayıplı olarak sıkıştırılmaktadır. Bu sayede, kayıpsız ve kayıplı sıkıştırma yöntemlerinin en uygun yönlerini bünyesinde barındıran melez bir hiperspektral veri sıkıştırma yöntemi geliştirilmiştir.

Farklı seyrek optimizasyon modelleri bulunmaktadır. Hiperspektral görüntü sıkıştırma başarımı ile ilgili seyrek gösterimlerin bağıl analizne de yer verilen çalışmada, çevrimiçi öğrenme tabanlı hiperspektral görüntü sıkıştırma modları iki farklı seyrek gösterimle sunulmaktadır. İki veri kümesi için hiperspektral görüntüler, üç seviye dalgacık dönüşümüyle izgel ilintisizleştirilerek sıkıştırılmaktadır.

Bu çalışma, iki tür veri kümesinden elde edilen (AVIRIS ve HYPERION) iki farklı hiperspektral veri üzerinde sonuçların alınmasını sağlamıştır. Ortalama Kare Hata (MSE) işlemine dayalı olarak belirlenen PSNR değeri, sonuç başarımlarının karşılaştırılması amacıyla kullanılmaktadır.

Bu tezde, verilerin mümkün olduğunca içsel bağıntısını kullanmak için tamamen veri tabanlı tekniklerden (sözlük öğrenme tabanlı seyreltik gösterimler) ve sabit katsayı dönüşümü (wavelet / DCT) temelli algoritmalarından yararlanarak dengeli bir hiperspektral görüntü sıkıştırma yaklaşımı önermekteyiz. Bu bağlamda, hiperspektral veriler tam rekonstrüksiyon elde etmek için tamsayı dalgacık dönüşümü temelli filtre bankaları kullanılarak spektral olarak ilintisizleştirilir. Spektral olarak ilintisizleştirilen verilerin, yüksek bant kısımları JPEG2000 standardıyla kodlanacak şekilde sıkıştırılırken, düşük bantlı veriler için çevrimiçi sözlük öğrenme çerçevesini kullanarak seyrek bir gösterim elde edilir.

Tezin katkısı, veriye dayalı uyarlanabilir katsayılı yaklaşımlar ile veriden bağımsız, sabit katsayılı süzgeç temelli yaklaşımların melez ve yenilikçi bir yaklaşımla harmanlanarak yeni bir hiperspektral veri sıkıştırma yöntemini ilk kez öneriyor oluşudur. Böyle bir yaklaşımın arkasındaki ana motivasyon, her iki yöntemin de hiperspektral görüntü sıkıştırma amaçları için yararlanılmasıdır.

Hiperspektral görüntülerin kayıplı sıkıştırılması için ayırt edici bir çevrimiçi sözlük öğrenme yöntemine dayanan seyrek kodlama algoritması önerilmiştir. Değişken sayıda sıfır olmayan sözlük unsurlarının etkileri de analiz edilmiştir. Sonuçlar, önerilen çevrimiçi öğrenme temelli seyrek kodlama algoritmasının, PSNR değerleri bakımından



daha iyi performans gösterdiği için, daha yüksek veri hızları için kullanılabilirliğini göstermektedir. Ayrıca, sıfır olmayan sözlük öğelerinin sayısının bir ön analizinin sıkıştırma yaklaşımının başarımını artırabileceği değerlendirilmektedir.





## 1. INTRODUCTION

In recent years the focus in several areas in the image processing has been increased. Remote sensing is the most important of these areas to carry out accuracy recording on sensed energy in many wavelength bands (Jin et al., 2005; Puri et al., 2014). Hyperspectral images combine the strengths of digital images and spectroscopy. A hyperspectral camera captures the light density for a big amount of neighbouring spectral bands. It can get accurate details of objects located in scenes through the uninterrupted spectrum owned by per pixel in the hyperspectral images (Url1).

In order to deepen our knowledge of the earth, it is necessary to obtain more comprehensive and more accurate information about it. So it is necessary to find means to monitor and control remotely especially from space to difficult-to-access places on the surface of the earth. Satellite images, and especially hyperspectral images, are important sources of data for many fields of different sciences. Satellite images cover a large area on the surface of the earth that is invisible to human eyes or other technologies. The term remote sensing was first used in the 1960s. It principally linked the study of the earth's surface and its biosphere. Satellite of different altitude are used to monitor the earth (Eismann, 2012).

Hyperspectral imaging (HSI) is a part of remote sensing technology for space reconnaissance and earth surveillance purposes (Goetz, 2009; Eismann, 2012). Being a spectral imaging method HSI acquires reflection data from objects in hundreds of narrow adjacent electromagnetic spectral bands. Hence, the acquired data may be visualized as a three-dimensional matrix of radiation or reflection values. It has two dimensional spatial and one-dimensional spectral components. A sample HS image data cube (3D matrix) is shown in Figure 1.1.

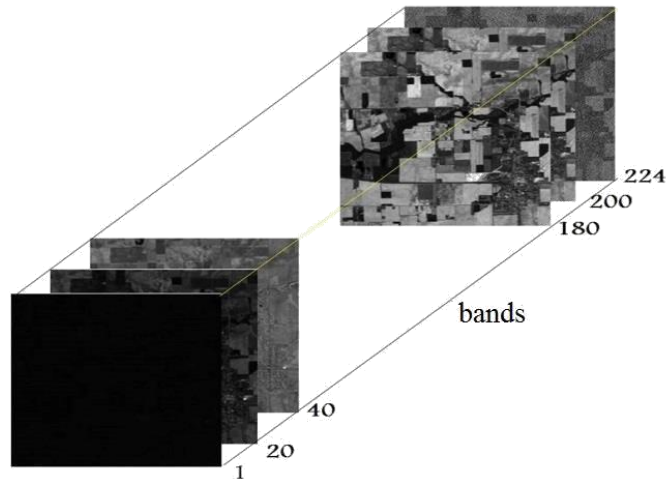


Fig. 1.1. A hyperspectral data cube sample (Low Altitude). The data cube is formed by a stack of two dimensional band images where bands make up the spectral component of the data.

Hyperspectral images compared to the regular visible range camera images can provide more abundant and accurate information of the scenes. Hyperspectral images provide insight about the chemical composition of the objects under consideration thanks to its spectral content.

Hyperspectral images come with the cost of huge data size. These massive data volumes strain storage and transmission strength of the present system (Romines, 2006). NASA's Airborne Visible Infrared Imaging Spectrometer (AVIRIS), for example, can produce a data size of around 16 Gigabytes in every day. Thus, there is an indispensable need of an efficient way of data compression which possibly exploits the correlation within the spectral and/or spatial content of the hyperspectral imagery.

There are many hyperspectral image compression techniques in the remote sensing literature (Ngadiran et al., 2010; Karami et al., 2010; Nallathai et al., 2013, Christophe, 2011). Handling hyperspectral data as a 3D cube and applying 3D compression technique that is an immediate extension of 2D technique is one of them. 3D Set Partitioning In Hierarchical Trees (SPIHT) and 3D JPEG 2000 are samples of these methods. Unlike the first method, where 3D hyperspectral data cube is compressed directly, in the latter approach, compression method is implemented to de-correlate the 3D data cube in the spectral dimension and the method is followed by 2D spatial

compression (Ramakrishna et al., 2005; Christophe, 2011; Hassanzadeh and Karami, 2016).

Many compression approaches depend on transform based techniques, such as Discrete Wavelet Transform (DWT) (Lee et al., 2005; Yang et al., 2007; Tang et al., 2003; Huang et al., 2004; Ramakrishna et al., 2006 and Christophe, 2011), and Discrete Cosine Transform (DCT) (Wang et al., 1998). The disadvantage of the transform based compression techniques is that the algorithm does not take into account the content of the data under consideration. As such, fixed filter coefficients are used to compress the hyperspectral imagery without considering the inherent characteristics of the data to be compressed. On the contrary, dictionary and sparse representation based approaches aim at using filter coefficients that adapt to the specific content of the hyperspectral data to be compressed (Ülkü and Töreyn, 2015a).

Dictionary and sparse representation based algorithms were recently proposed for HSI compression and analysis purposes (Ülkü and Töreyn, 2015a; Huo et al., 2012; Wang et al., 2014; Ülkü and Töreyn, 2015c) The important aspect of the sparsity based compression techniques is that a dictionary is learned in accordance with the input data. In addition, a sparse representation based on the learnt dictionary is achieved yielding a tightly coupled representation of the data to be compressed.

Apparently, transform based techniques and data-driven approaches, like dictionary based methods, may be considered as two extreme approaches for HSI compression. The transform based techniques compress the data using filters that are totally independent from the data itself. On the other hand, dictionary learning based methods are fully data-driven.

### **1.1 Contribution of the Thesis**

In this thesis, we propose a balanced hyperspectral image compression approach by leveraging fully data-driven techniques (dictionary learning based sparse representations) and fixed coefficient transform (wavelet / DCT) based algorithms, to exploit the inherent correlation of the data as much as possible. To that extent, hyperspectral data is spectrally decorrelated using integer wavelet transform based filter banks, in order to achieve perfect reconstruction. Spectrally decorrelated data is further compressed in such a way that the high-band data is coded with JPEG2000 standard (Töreyn et al., 2015), whereas a sparse representation is obtained for the low-band data using an online dictionary learning framework (Ülkü and Töreyn, 2015b).

The contribution of the thesis is that a hybrid hyperspectral data compression method blending a pure data driven dictionary learning framework with a fixed coefficient integer wavelet transform based spectral decorrelation mechanism is proposed for the first time. The main motivation behind such an approach is to exploit the advantages of both methods for hyperspectral image compression purposes.

## **2. LITERATURE REVIEW**

In this chapter, a survey on the compression of hyperspectral imagery is presented. The chapter starts with a review on lossy compression methods for hyperspectral imagery. It is followed by a discussion of techniques on lossless hyperspectral image compression. Other hyperspectral data compression techniques leveraging lossless and lossy approaches in the literature, such as, distributed source coding based methods are also reviewed. The chapter concludes with a discussion on sparse representations and dictionary learning based methods, as lossy compression approach presented in the thesis is substantially based on sparse representations.

### **2.1 Lossy Compression of Hyperspectral Images**

From the title, it seems to be different from our subject, but what concerns us is touched by a researcher from the sparse representation as well as how to handle the dictionary learning in hyperspectral images (Ülkü and Töreyn, 2014). Gave a description of the process of using the dictionary learning which in turn is the process of data loss, was a result of the Peak Signal to Noise Ratio (PSNR) indicated without utilized the dictionary learning 31.49, On the contrary, this work in which the value of PSNR (infinity) and after using the dictionary learning and three levels the researcher gets different values show from 44 to the level of first and ranging to 104 for the third level that describes the impact of the dictionary learning on the images compression and its quality. And the fact that the loss caused many problems during the classification process can be overcome using the hybrid compression, which in turn provides the features of the image to obtain a good and accurate classification after compression (Lee et al., 2015). But others adopted some methods and after dividing the hyperspectral images into several layers of pixels, which are prone to applying Spectral Angle Mapping (ASM) and Principal Component Analysis (PCA). This process subject to segmentations with wavelet transform (WT) (Tamhankar and Fowler, 2007). But (Zhou et al., 2006) have another opinion which is to keep the basic information in the images and the intended edges, which is applied to spatial decorrelation. In



(Alaydin and Toreyin, 2016) their approach depends based on the value of bit rate this mean getting the best quality of performance that should has low BPS, Before use the dictionary learning step over the low-sub-band data, adopted by the above author one level of WT The higher subband is further compressed in a lossless approach utilizing JPEG2000. Regarding the dictionary learning is considered a lossy manner during data compression, On the contrary, the spectral decorrelation in our work carried out by 6 types of filter (Haar,  $9\sqrt{7}$ ,  $5\sqrt{3}$ ,  $9\sqrt{3}$ ,  $6\sqrt{2}$  and  $5\sqrt{11}$ ). With three levels WT. As well the higher sub-band is compressed using JPEG2000. Sparse representation plays an important role in the process of removing noise from spectral images (Lu et al., 2016). its use in this aspect to overcome the relapse in hyperspectral images resulting in noise in the images (Christophe et al., 2005; Acito et al., 2011; Lin and Bourennane, 2013). Spectral image compression process has proved in these days a flexible environment to work in the field of research. As we mentioned above that the spectral images consisting of three dimensions, as well as containing a set of images or scenes similar but different wavelength (Puri et al., 2014). It can be obtained or picked many ways the first of sensors such as NASA's (Shahriyar et al., 2016). Because of technical possibilities possessed by the spectral images taken advantage of widespread use in many areas such as disclosure and determine the analogy of the surface (Tang and Pearlman, 2006). The compression type above can be two types of compression lossy, lossless as we said earlier that the first in which some information is lost after the compression process, while the second is information retrieval entirely. It's not in favour of the second (lossy) because some data loss leads to loss of the main factor in the spectral images and is responsible for the discovery processes as well as identification and this factor is called spectral signatures. Well, there are two ways to spectral image compression, the first dealing with the overall size of the cube, in other words, compression is three-levels in order to get the highest possible proportion of this process (Toreyin et al., 2015). The second relies mainly on the spectral correlation (Prasad et al., 2011).

## **2.2 Lossless Hyperspectral Image Compression and Decorrelation approaches**

In this part we will present two papers that almost has a little similarity correspond to this work, the first one that focused in estimate the performances by utilized the integer-coefficient DWT filters but the author also focused on compression ratio and the influence of the filters which we mentioned them above (Toreyin et al., 2015).

While in our work we used these filters in many operations and the important one compression. And the second part to take the process used in the process of calculating bit rate sample by used the JPEG2000 method for getting the lossless compression of the high sub-band in all levels WT. But there are researcher follow other steps to get liken to original data, that means after the spectral image compression we get a few data loss of contents (lossless), In this approach it has been to rely on non-linear generalization of the statistical technique, popular technique for getting patterns in data of high dimension that mean based on PCA Which it has been applied to a set of images by auto-associative neural networks, researcher also touched on that image compression process and increase limited to the number of nodes in them , and the Nonlinear Principal Component Analysis (NLPCA) played a major role in the search being allowed to lose a minimal number of features (Licciardi et al., 2014).

the researcher proficient in the use of technology above depends on the statistical properties of the images and he proved through experience that the use of this technique is best to get a good outcome to the process of spectral image compression, as well as the calculations modest and uncomplicated (Wang et al., 1995). A new technique is considered at the time to get the images is not devoid of original data (lossless) and the experience was on the Landsat-TM data. There are some researchers followed styles in order to process the content above, which is used in linear prediction and some of them over the work stages so as to get rid of the impurities after the compression process (Roger and Cavenor, 1996). But there is another follow a new approach, a deep dealing with images spectral properties. This was done by taking advantage of the abundance of spectral in hyperspectral images, as well as relying on the existing correlation between neighbouring bands in the images mentioned above (Wang et al., 2007). Some used the same idea of redundancies of inter-band and depending on (Context-based, Adaptive, Lossless Image Codec) for getting the high performances from compression, as well as whereby it can reduce the bit rate compared to the rest research (Wu and Memon, 2000).

Lossless compression is predominantly carried out in two procedure, the first one Decorrelation in this point able to visible accordingly to first-order entropy decrease step in which the abundance or correlation of the data is isolated and a superfluity image is acquired. There are a lot of predictors are progressing for this aim. The second, Coding: This stage utilizes a coder that transitions the remaining image for a

result bit stream. Generally the algorithms of lossless compression in remote sensing environments employ just for spatial decorrelation (Memon et al., 1994).

There are different types of spectral decorrelation approaches likewise (KLT), (DWT), (DCT) and Vector Quantization (VQ) able to done by previous to 2- levels-compression (Galli and Salzo, 2004; Magli et al., 2004; Christophe, et al., 2008; Mielikainen and Toivanen, 2003; Aiazzi et al.,1999; Bilgin et al., 2000; Penna et al., 2006; Lee et al., 2002).

Every model or approach includes pros and cons. For example, KLT contains the better decorrelation efficiency; but, it is so complicated and there are necessarily for a large quantity of calculation energy, storage and time that gives a pointer it inappropriate with regard to spaceborne applications. Besides, VQ needs for lower time and least computation energy; however, compared with KLT it has minimum decorrelation performance. Resource demand of DCT is significantly less matched to prior of which; but, it presents a lossy transform that is unsuitable concerning with lossless image compression. Ultimately, DWT presents lossless and lossy transform that able to chosen by means of a user and accompanied by comparatively less complicated, low counting time and power need.

### **2.3 Lossy and Lossless Hyperspectral Image Compression**

Hyperspectral Images refer to the images that have a sufficient amount of spectral bands. Those bands mostly contain a kindly spectral abundance and spatial abundance. As mentioned above, the process of compressing hyperspectral images can be divided into two processes “lossless” approach such as (Mamatha and Singh, 2014; Töreyn et al., 2015b; Shahriyar et al., 2016). The other approach “lossy” such as (Ülkü and Töreyn, 2014; Conoscenti et al., 2016). In addition to the approaches followed there are many methods for both approaches, like Optimized for Spectral Unmixing (Karami et al., 2016) and other depending on Independent Component Analysis (Yang et al., 2014). The number of bands and the excessive flexibility found in hyperspectral images give the opportunity for many to work in the conversion between approaches, lossy to lossless and vice versa. In (Cheng and Dill, 2014) a lossless to lossy compression methods for hyperspectral images that depending on dual-tree Binary Embedded Zerotree Wavelet (BEZW) algorithm, The algorithm conforms with Karhunen–Loève Transform and DWT to obtain 3- levels integer reversible hybrid

transform and decorrelate data of a hyperspectral image. While in (Wang et al., 2009) the approach that followed Lossy-to-lossless hyperspectral image compression they suggest a modern transform way of multiplierless reversible time-domain lapped transform and Karhunen–Loève transform (RTDLT/KLT) for lossy-to-lossless hyperspectral image compression. Instead of using (DWT) in the spatial domain, RTDLT is utilizing for decorrelation.

Diminishing the abundance is consider the major target of the data compression( encoding information) algorithms. With a view to attaining this, an existent correlation in the images is possible to depend. Probably, generally utilized 2- levels image compression principles, like JPEG-LS or JPEG2000 at all events, look just the intra-band correlation. Accordingly, high inter-band correlation attends in hyperspectral images residues not take advantage of that outcome in low compression rates. Furthermore, so as to obtain best compression ratios the spectral correlation offer in the image must be traded on.

There are two major kinds of hyperspectral image compression approaches. The first is depending on 3- levels compression, which deals with the data or images as cube style. This is a type of compression modes possible to obtain top compression ratios. But, decorrelating the data in all three dimensions with one another, raises the hardware intricacy and demands a massive magnitude of processing energy and storage, which is commonly out of the question to be faced by spaceborne frameworks. Furthermore, the wanted time of processing is very loudly that it impossible contraction the data rate created through of hyperspectral sensors. So, 3- levels compression modes are mostly used for earth applications and comparatively tiny images like biomedical images (Penna et al., 2006; Schelkens et al., 2000; Dragotti et al., 2000).

#### **2.4 Distributed Source Coding Based Hyperspectral Image Compression**

Each compression process flaws and advantages that make many researchers search for techniques that give or produce high performance in hyperspectral image compression. One of these important technologies that have been introduced because of its effectiveness Distributed source coding (DSC), which some relied on to facilitate of some complicated calculations and the dynamic process between encryption and decryption (coder and encoder) through the control of correlation in various bands (Barni et al., 2005). However, in another work, have been exploited on the relationship

between DSC- wavelet and the process of combining DSC and intra-coding that the results were satisfactory as well as technical was convenient for the three-dimensional wavelet (Barni et al., 2005). Some researchers follow a bit of the same technique to exploit the correlation between pixels bands, with the use of technology ensures hyperspectral images efficiency by utilizing prediction model with wavelet interference. Tang et al. and Barni et al. (2005) suggest algorithm for lossless hyperspectral compression-based on multilevel coset codes. That depended on a block-based way, after the process of separation bands of images to a group of small separate blocks are processing or analysis of each block separately. This deal with blocks gives outstanding performance and is far from the complexity (Cheung and Ortega, 2009).

## **2.5 Dictionary Learning for Hyperspectral Image Compression**

The spatial resolutions of hyperspectral images are generally lower due to imaging hardware limitations. High resolution algorithms are more usable for getting superior resolutions. There are a numerous algorithms occur to obtain high resolution Hyperspectral images from minimum resolution images gained in different wavelengths. The most commonly algorithms is sparse representation-based algorithms that utilize dictionary learning approaches. According to (Şımşek and Polat, 2015) they are study of framework is improvement of indicate which dictionary learning algorithm achieve to better high-resolution images. The results show that ODL algorithm out KSVD in terms of both reestablishment quality and processing times.

Many algorithms like K-SVD (Elad and Aharon, 2006), Non-local means (Buades, et al., 2005) and block-matching and 3- levels filtering (BM3- levels) (Dabov et al., 2007) their target sophisticated about 2- levels image denoising. These approaches able to immediately employed for denoising of HSI by denoising every band image individually. But, taking into account the bands to be separate restricts performance. (Qian et al., 2012; Maggioni et al., 2013) denoise HSI through seeing 3- levels cubes of the HSI rather than the 2- levels patches of a conventional image to recovery, however, these modes disregard the rising correlation over spectra and restrict their accomplishment.

A numerous approaches depend on Wavelet and PCA for Hyperspectral image denoising. In study of (Atkinson, et al., 2003; Othman and Qian, 2006) have been both suggested wavelet-based HSI denoising algorithms. In another study conduct by (Chen and Qian, 2009; Chen and Qian, 2009) submit implementing of dimensions decreases and HSI denoising by using of wavelet retraction and principal component analysis (PCA). (Lam et al., 2012) are using of principal component analysis for dimension decreases in the spectral domain and then implemented denoising in local spatial proximity to further developed denoising outcomes. By the findings from (Karami, et al., 2011) minimized the noise of Hyperspectral image by using their Genetic Kernel Tucker Decomposition. (Guo et al., 2013) denoised the hyperspectral image depended on a high-order rank-1 tensor decomposition. Furthermore, (Wang et al., 2010; Wang and Niu, 2009) were used an alternative hyperspectral anisotropic diffusion scheme to denoise Hyperspectral image. In deep point of findings, (Yuan et al., 2012) used spatial-spectral adaptive total kinds of model for their denoising forms. In another term, (Zhong and Wang, 2013) together model and uses spatial and spectral reliance in a unified probabilistic scope by multiple-spectral-band conditional random areas. So, (Zhang et al., 2014) explored the low-rank property of hyperspectral image for image restoration. Several methods utilized both spatial and spectral data. Whereas, nobody has exploited the non-local self- resemblance offer in hyperspectral image of natural scenes.

In study by (Qian and Ye, 2013) submitted the non-local self-similarity and spatial-spectral framework of hyperspectral image towards a sparse representation structure, but their method used a commonly 3- levels dictionary made up from 3- levels DCT and 3- levels OWT, that not to be appropriate for some conditions of intended scene.

Finely, (Peng et al., 2014) conducted a hyperspectral image denoising method depending on decomposable non-local tensor dictionary learning, due to their model did not deal with the neighboring non-local self-similarity towards account.

## **2.6 Sparse Representation in image processing for Hyperspectral Data**

Sparse representation has found many applications In image processing missions like image classification (Bahrapour et al., 2016), image denoising , deblurring, inpainting (Elad et al., 2010) image restoration (Mairal et al., 2008). Compression of a fixed field of images or more public images utilizing sparse representation can be found in (Bryt and Elad, 2008; Skretting and Engan, 2011). In (Ülkü and Töreyn,

2014) a lossy compression of hyperspectral images utilizing sparse representation was presented. Newly, sparse representation (SR) term has been explained to be a strong tool in digital signal processing (Li et al., 2013; Zhang et al. 2015). Mostly, natural signals are looked to be sparse and can be performed by sparse coefficients (vectors) through a dictionary in the SR pattern. The sparse coefficients include just a few nonzero entries; consequently, the information of original signals is usually compressed for the small nonzero values of sparse coefficients. The SR compression manner has been used to 2-D image compression in (Skretting and Engan, 2011) by sparsely representing nonoverlapping image patches through an offline dictionary. The gained sparse coefficients are quantized to integers and then converted into a bit stream by the entropy coding technique. The SR compression way enables prolonged to compression of HSIs, ever after spectral signatures of HSI pixels can be sparsely represented according to (Li and Du, 2014; Fu et al., 2016; Fang et al., 2016). The basic manner is to separately compress every HSI pixel by sparsely representing the pixel's spectral signature through an appropriate dictionary. Distinct the SR-based 2-D image compression (Skretting and Engan, 2011), which learns an offline dictionary for different images, the HSI compression demands a data-dependent dictionary on account of the big diversity of HSIs. Sub dictionary depend on dictionary structure approach (Dong et al., 2013), which has a bit complication and leads to sparser representation which may be utilized for SR compression. The on the top of SR method for HSIs compression can be called the pixelwise SR (PWSR) approach. However, the PWSR method overrides the spatial correlation of HSI pixels, i.e., neighboring pixels generally performed the same material and share the comparable spectral signatures. In (Eldar et al., 2010; Tang and Nehorai, 2010) they are offered simultaneous SR of correlative signals (i.e., similar vectors) with the row-sparse coefficients can regain signals with higher sparsity scale (i.e., sparser coefficients) contrasted with the SR of the single. This is due to the former combine's contextual information of signals into the model. Thus, the spatial correlation of HSI pixels is substantial for the SR compression, when neighboring HSI pixels might possibly be correlative signals and can be represented by sparser coefficients to get better the compression performance. Solving problems related to the process sparse coding with hyperspectral image compression and dictionary learning require a stand against the main problems and difficulties and to overcome them.

The goals of the sparse coding are to build the brief representation for the data (pre-process data). Depending on this kind with using pre-specified number of atoms can be used to generate a data spot of the dictionary learning model the input data (Xie et al., 2013; Bao et al., 2016). Using sparse model can obtain the lowest possible number of non-zero elements to represent data.

thesis. The hybrid approach, which comprises lossless spectral decorrelation, lossless compression of high-band data and sparse representation based lossy compression of the low-band data steps, benefits from advantages of both lossless and lossy schemes. Dictionary-based learning approaches became very a popular in image processing and others fields (Lee et al., 2006; Mairal et al., 2010). In dictionary-based learning approaches, through a little of dictionary elements can represent the signals. In lieu of depending on previously prepared dictionaries or specific filter coefficients for performing compression objective, dictionary learning-based way yields the best achievement in an expression of compression ratio and image fineness (Aharon et al., 2006).

Algorithms which are depending on repeat batch operating guarantee training by getting the whole dataset at every repetition that produces such algorithms feeble for big datasets (Bousquet and Bottou, 2008). On the grounds that the substitutional kinds of algorithms, dictionary learning algorithms whose based on random approximations are useful for big datasets. By performing sparse coding approaches for dictionary learning aims on hyperspectral imagery is survived previously (Charles et al., 2011). Dictionary elements and coefficients identical to those are supposed to carry on (either positive or negative) values in (Charles et al., 2011).

The sparse coding optimization issues are presented as a regularized least-squares objective function based on a series of standards on the dictionary elements. The solution to the trouble is acquired utilizing an optimization package principally intended for  $l_1$ -regularized regression troubles (Koh et al., 2007).

The convex optimization issue which is utilized for updating procedure permits detachable chains in the new dictionary columns. Thus, it is ensured that the point of the concourse is carried out at the universal optimum stage (Bertsekas, 1999).

Dictionary learning is presented as a solution issue wherever a smooth non-convex objective function is optimized through a convex set pleasurable as a series of circumstances. This optimization issue is fixed based on the online algorithm. By



considering is a partially of the online algorithm, a quadratic surrogate function of the experimental cost is reduced within every iterative tread. Manner is proved to converge to a fixed point of the cost function with eventuality one (Mairal et al., 2009).

### 3. METHODOLOGY

In this chapter, the proposed compression method is presented, in detail. The method is comprised of three stages, namely, i. spectral decorrelation of the hyperspectral data using integer wavelet transform, ii. two dimensional lossless compression of high subband images, iii. obtaining a sparse representation for the low subband data block. Details of the stages are presented below.

#### 3.1 Spectral Decorrelation

The data (cube) is decorrelated in the spectral direction using integer wavelet transform. This results in low and high subband data blocks (cf. Figure 3.1).

Let  $X \in \mathbb{R}^{n_l \times n_s \times n_b}$  represent the hyperspectral image, where the number of bands in the hyperspectral cube is represented by  $n_b$ , the number of lines in the hyperspectral cube is represented by  $n_l$ ,  $n_s$  represents the number of samples in the hyperspectral cube.

Let

$$x_{i,j}[k] = [X[i,j,1], \dots, X[i,j,n_b]] \quad (3.1)$$

be a vector of hyperspectral data values for all the bands,  $k=1, \dots, n_b$ , at the  $(i,j)$ -th spatial location, where,  $i=1, \dots, n_l$ , and  $j=1, \dots, n_s$  (cf. Figure 3.1).

As the name suggests, spectral decorrelation step aims at decorrelating the spectral content using integer wavelet transform based filter banks (Chrysafis and Ortega, 2000; Chui et al., 1998). This provides a perfectly reconstructable decomposition of

**Table 3.1** High pass filters for Various Integer Wavelet Transforms

Filter	Values	
Haar	$h_0[k] = \left\{ \frac{1}{\sqrt{2}}, -\frac{1}{\sqrt{2}} \right\}$	(3.2)
9-7	$h_0[k] = \left( \frac{1}{16}, \frac{1}{8}, -\frac{1}{4}, -\frac{1}{2}, \frac{1}{2}, \frac{1}{8}, -\frac{1}{16} \right)$	(3.3)
5-3	$h_0[k] = \left( \frac{1}{\sqrt{2}}, -\frac{1}{\sqrt{2}} \right)$	(3.4)
9-3	$h_0[k] = \left( -\frac{1}{2}, \frac{1}{2}, -\frac{1}{2}, \frac{1}{2} \right)$	(3.5)
2-6	$h_0[k] = \left( \frac{1}{8}, \frac{1}{8}, -\frac{1}{4}, -\frac{1}{4}, \frac{1}{8}, \frac{1}{8} \right)$	(3.6)
5-11	$h_0[k] = \left( \frac{1}{\sqrt{2}}, \frac{1}{\sqrt{2}}, \frac{1}{\sqrt{2}}, \frac{1}{\sqrt{2}}, \frac{9}{\sqrt{2}}, \frac{1}{\sqrt{2}}, \frac{1}{\sqrt{2}}, \frac{1}{\sqrt{2}}, \frac{1}{\sqrt{2}} \right)$	(3.7)

**Table 3.2** Low-pass filters for Various Integer Wavelet Transforms

Filter	Values	
Haar	$l_0[k] = \left\{ \frac{1}{\sqrt{2}}, \frac{1}{\sqrt{2}} \right\}$	(3.8)
9-7	$l_0[k] = \left( \frac{1}{16}, \frac{1}{8}, \frac{1}{4}, \frac{1}{2}, \frac{1}{2}, \frac{1}{8}, \frac{1}{16} \right)$	(3.9)
5-3	$l_0[k] = \left( \frac{1}{\sqrt{2}}, \frac{1}{\sqrt{2}} \right)$	(3.10)
9-3	$l_0[k] = \left( \frac{1}{2}, \frac{1}{2}, \frac{1}{2}, \frac{1}{2} \right)$	(3.11)
2		
-		
6		
5-11	$l_0[k] = \left( \frac{1}{\sqrt{2}}, \frac{1}{\sqrt{2}}, \frac{1}{\sqrt{2}}, \frac{1}{\sqrt{2}}, \frac{9}{\sqrt{2}}, \frac{1}{\sqrt{2}}, \frac{1}{\sqrt{2}}, \frac{1}{\sqrt{2}} \right)$	(3.12)
	$l_0[k] = \left( \frac{1}{8}, \frac{1}{8}, \frac{1}{4}, \frac{1}{4}, \frac{1}{8}, \frac{1}{8} \right)$	(3.13)

the original data,  $X$ , into two (or more depending on the number of levels) subbands in the spectral dimension. The decomposition is composed of convolution with low(high)-pass filter,  $l_0[k](h_0[k])$ , followed by decimation (cf. Figure 3.2). As a result,  $x_{i,j}[k]$  for each and every line and sample location, is decomposed into low-band,  $x_{i,j}^l[k]$ , and high-band,  $x_{i,j}^h[k]$ , components. In order to assess the efficacy of various integer wavelet transform filters on spectral decorrelation, this decomposition is realized using different wavelet transform filterbanks which are presented in Tables 3.1 and 3.2.



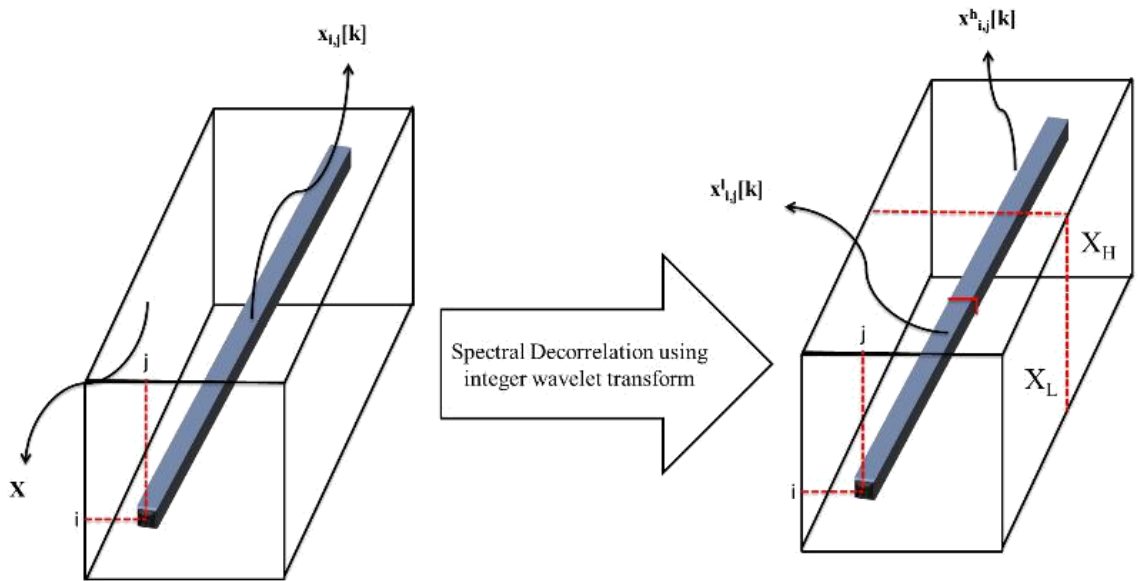


**Figure 3.1** The hyperspectral data,  $X$ , is decomposed into low,  $X_L$ , and high,  $X_H$  subband blocks, in the spectral dimension. This is achieved by decomposing  $x_{i,j}[k]$  for each line and sample,  $(i,j)$  location, into low-band,  $x_{i,j}^l[k]$ , and high-band,  $x_{i,j}^h[k]$ , components.

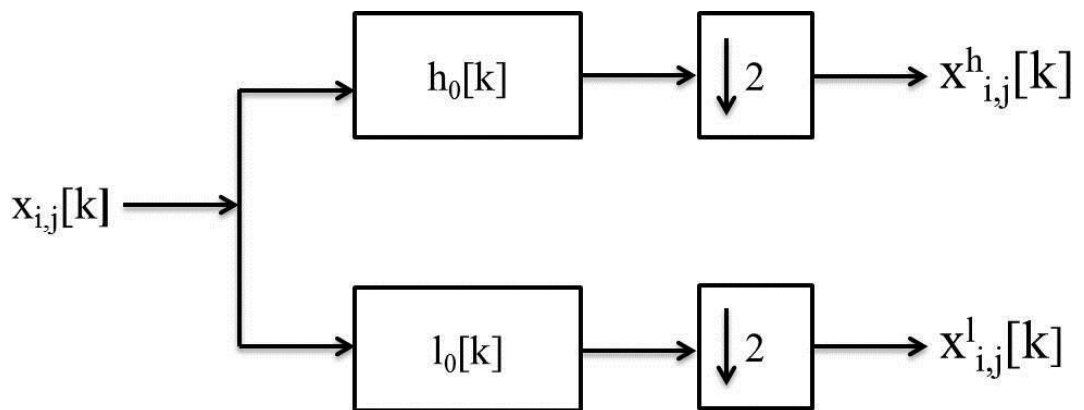


**Figure 3.2** Single-level integer wavelet transform. Each  $x_{i,j}[k]$  corresponding to the spectral content at location  $(i,j)$  is decomposed into two components, namely,  $x_{i,j}^l[k]$ , and  $x_{i,j}^h[k]$ .

This decomposition, in turn, decomposes the whole hyperspectral data,  $X$ , into two subband blocks, namely, low-band,  $X_L$ , and high-band,  $X_H$ , data blocks, where,

$$x_{i,j}^l[k] = [X_L[i,j,1], \dots, X_L[i,j, \frac{K}{2}]] \quad (3.14)$$

and

$$x_{i,j}^h[k] = [X_H[i,j, \frac{K}{2} + 1], \dots, X_H[i,j, K]] \quad (3.15)$$

and is even.

Once the hyperspectral data is spectrally decorrelated using integer wavelet transform, the high-band data block,  $X_H$ , composed of high subband images, and low-band data block,  $X_L$ , composed of low subband images are processed separately, in order to fully exploit the redundancy present in the hyperspectral imagery.

### 3.2 High subband images are compressed using JPEG2000 codec in lossless mode

As the high-band data block,  $X_H$ , is composed of high-band components,  $x_{i,j}^h[k]$ , that block is already sparse with very few number of non-zero values. Such a sparse and highly correlated data may be compressed using lossless image compression techniques that are already mature, such as JPEG2000 codec (Christopoulos et al., 2000). There are studies in which JPEG2000 codec is utilized for hyperspectral data compression (Penna et al., 2005).

Different than other techniques in the literature, in this work, we compress the 2 many-high subband images in (3.15) using JPEG2000 codec in lossless mode. In particular, the high-band subimages,  $X_H[:, :, k]$ , for  $k = 2 + 1, \dots, \dots$ , are compressed using

JPEG2000 codec in lossless mode, where ‘:’ stands for all values in the range of that particular dimension, namely,  $i=1, \dots, n_l$ , and  $j=1, \dots, n_s$ .

### 3.3 Low Subband Data Block is processed to obtain a Sparse Representation

As opposed to the high-band data block,  $X_H$ , the low-band block  $X_L$  is composed of low-band components,  $x_{i,j}^l[k]$ , which, depending on the data, is far from being sparse by default. In order to obtain a sparse representation, the low-band block is processed using dictionary learning based techniques.

The motivation behind utilization of sparse representation based compression schemes is that, these methods are shown to yield better compression performance as compared with other state-of-the-art approaches in hyperspectral image compression (Ülkü and Töreyn, 2015b).

#### 3.3.1 Sparse Coding

Sparse representations of signals have drawn large attention in the last period. The sparse model is a sturdy way to portray signals depending on the sparsity and

abundance of their representations (Mairal et al., 2008). As we have stated previously that the structure of the hyperspectral images is a spatial and spectral and under its banner gangs. To solve a big problem, such as image compression spectral problem we should look for systems or models. So in this area has been to rely on the sparse coding. The sparse coding deal with signal vectors assumptions they're an integral part of the subspace, In the end, the signals may after using the sparse coding trend to showing as linear transform (Wang and Celik, 2016). And it is considered as ways of the compression methods. Sparse coding: This procedure indicates to returning the coefficient vectors where a dictionary  $D$  is specified. Sparse coding is fixed in an individually approach when for every sample  $x$  in equations (3.16 and 3.17), its coefficient vector  $\alpha$  possible got separately in the else sample. A greedy algorithm like matching pursuit (Mallat, and Zhang, 1993) in addition to OMP (Davis et al., 1994) possible used when  $l_0$  norm is utilized to encourage sparsity within coefficient vectors. Efficient algorithms, like Basis Pursuit (BP) (Chen et al., 2001). The procedure of sparse coding, generally indicated to as “atom decomposition”, call for solving.

$$(P_0) \quad \|x\|_0 \text{ subject to } y = Dx \quad (3.16)$$

or

$$(P_0, \epsilon) \quad \|x\|_0 \text{ subject to } \|y - Dx\|_2 \leq \epsilon \quad (3.17)$$

These are algorithms (greedy) that choose the dictionary vectors alternately. Together (3.16) and (3.17) are readily processed by alteration the cessation base of the algorithm.

The Basis Pursuit (Chen, et al., 2001) proposes a convexification of the issues presented in (3.18) and (3.19), by substituting between  $l_0$  -norm and  $l_1$  -norm.

### 3.3.1.1 Least Absolute Shrinkage and Selection Operator

Last decade, the LASSO approaches have become common approaches for parameter assessment and mutable chosen due to their ownership of shrinking several of the patterns coefficients to precisely zero (Lu and Su, 2016). LASSO recession modes are openly used in domains with huge datasets, such as genomics, where dynamic and fast algorithms are the major (Friedman et al., 2010). The LASSO is not solid to the high connection among predictors and will randomly choose one and eliminate the others

and shot down when all predictors are similar (Friedman et al., 2010). The LASSO sanction expects a lot of points to be close to zero, and only a little subdivision to be bigger (either positive or negative). The LASSO estimator (Tibshirani, 1996), utilizes the  $\ell_1$  penalized least squares criterion to get sparse outcomes to the (3.27). The  $\ell_1$  penalty support the LASSO to together regularize the least squares fit and shrink several ingredients o lasso to zero for several appropriate selected  $\lambda$ .

### 3.3.1.2 Basis Pursuit

The basis pursuit (BP) algorithm (Chen et al., 2001) proposes the replacement of the  $\ell_0$ -norm in (3.16) and (3.17) with an  $\ell_1$ - norm. So solutions of:

$$(P_0) \quad \|x\|_1 \text{ subject to } y = Dx \tag{3.18}$$

in the accurate representation issue, and

$$(P_0, \epsilon) \quad \|x\|_1 \text{ subject to } \|y - Dx\|_2 \leq \epsilon \tag{3.19}$$

In (3.18), guide to the BP representation. A solution of (3.19) amounts to linear programming and a good solvers for the issues occur. The approximate format (3.19) guides to a quadratic programming constructing, and still, there work out functional solvers for that problems.

In returns the outcome of  $x$ , for the (neither positive and negative) coefficients match to atoms of the dictionary,

We are able to utilize the indexes of the nonzero ingredients of  $x$  to recognize the columns of  $D$  that are indispensable to replicate the signal. This set is a foundation of a representation. Utilizing 1-norm permit us to specify a cost for every atom which used in the representation.

### 3.3.2 Dictionary Learning

Recently, the focus of many researchers and practitioners in the field of processing images and signals on the sparse representation, for the obvious emergence in many important applications, which is the heart of the work in image processors and signal, like denoising of image (Elad and Aharon, 2006), face recognition (He et al., 2013;



Wang et al., 2015) and super-resolution reconstruction (Zhang et al., 2015; Yang et al., 2010). That has the ability to appear as little atoms of a specific over-complete dictionaries (Candes et al., 2011).

The technique of dictionary learning is considered explicit technique. Depending on the below equation each training for images can be divided into nested spots. We should compute sparse basis and dictionary learning  $D$  for every input.

$$\min_{\alpha} \frac{1}{2} \|x - D\alpha\|^2 + \lambda \|\alpha\|_1 \quad (3.20)$$

where  $T$  is number of iterations,  $x$  input as sparse basis and  $\alpha \in \mathbb{R}^k$ .

Some techniques can be used for the purpose of implementing the algorithm for the dictionary learning like Orthogonal Matching Pursuit (OMP) and Alternating Direction Method of Multipliers (ADMM).

### 3.3.3 Sparse Coding and Dictionary Learning

Dictionary learning based methods become popular among researchers working on hyperspectral image compression (Wang and Celik , 2016; Wang et al., 2014). The main idea behind dictionary-learning-based methods is to represent the data using minimum number of dictionary elements.

By utilizing the  $\ell_0$  norm concerning data that represent nonzero vector elements. The core of our topic is getting sparse representation is done by reducing the value of  $\ell_0$  (Elad et al., 2010). Possible comparison between the previous norm and the norm more flexible purpose is to provide more for the concept of the sparse and possible to call this norm  $\ell_1$  depending upon the results can be obtained and efficient solutions able to solve a lot of problems related to sparse coding (Elad et al., 2010). Many studies divided representation algorithm the sparse into several categories: Relax convex, greedy algorithms, and methods of combinatorial. On the other views sparse decomposition algorithms are mostly separated into two parts: greedy algorithms and convex relaxation algorithms (Zhang et al., 2015; Tropp, 2006; Tropp et al., 2006; Cheng et al., 2013).

But there is another opinion to divide the sparse representation also into three sections can enumerate as follows: greedy pursuit algorithms,  $\ell_p$  norm regularization based

algorithms, and iterative shrinkage algorithms (Yang et al., 2009). Can underestimate the norm  $\ell_0$  because the main objective of greedy pursuit algorithms. The Matching Pursuit (MP) considered one of the fundamentals that are dealing with recent algorithm (Davis et al., 1994).  $\ell_p$  is decreased more If compared with the  $\ell_0$  norm. Through some research and found that the strongest and most appropriate example for  $\ell_p$  norm - regularization - based techniques is Basis Pursuit (BP)( Chen et al., 2001). After all of the above cannot fail to pose another kind and is important in the representation process above class as well as it is very important in our work and followed by its equation with a basis pursuit equation, is type called Least Absolute Shrinkage and Selection Operator (LASSO) (Tibshirani, 1996). That we proposed it as representation- based hyperspectral image coding.

In sparse-coding-based hyperspectral image compression using the next sparse representations:

- Least Absolute Shrinkage and Selection Operator.
- Basis Pursuit.

In this thesis, the low-band block  $X_L$  is processed using dictionary learning based techniques in such a way that,  $x_{i,j}[k]$ 's are used to form a dictionary,  $D \in \mathbb{R}^{n_b \times f}$ , where  $f$  denotes number of columns in the dictionary, and  $n_b = 2$ . The matrices  $A$  and  $B$  are considered for updating the dictionary where  $A \in \mathbb{R}^{f \times f}$  and  $B \in \mathbb{R}^{n_b \times f}$ ,  $T$  be the number of iterations,  $E \in \mathbb{R}^{f \times 1}$  be the error,  $\lambda \in \mathbb{R}$  be the regularization parameter, and  $\alpha \in \mathbb{R}^f$  be sparse coefficients. In addition to above information that mentioned about cubes (Table 4.1) and as we proposed in our introduction the following Parameters that are used in the analysis are defined as  $n_b$  It symbolizes the number of bands in the hyperspectral cube,  $n_l$ ,  $n_s$  symbolizes the numbers of rows and columns (lines and samples), and the number of the columns in dictionary represented in the  $f$ . assume  $D_0 \in \mathbb{R}^{n_b \times f}$  be the initial dictionary,  $A \in \mathbb{R}^{f \times f}$  and  $B \in \mathbb{R}^{n_b \times f}$  be assist matrices utilized in process updating the dictionary,  $T$  is number of iterations,  $E \in \mathbb{R}^{f \times 1}$  be the error,  $\lambda \in \mathbb{R}$  be the regularization parameter, and  $\alpha \in \mathbb{R}^f$  be sparse coefficients and The below equation refer to empirical cost function.

$$F_T(D) = \frac{1}{T} \sum_{t=1}^T \| \Sigma^T - D \alpha \|^2 \quad (3.21)$$

where  $V = \{v_1, \dots, v_T\}$  in  $\mathbb{R}^{n_b \times n_f \times T}$  is the finite training set,  $D$  in  $\mathbb{R}^{n_b \times f}$  is the dictionary. Sparse Coding and Dictionary Update Equations Corresponding to LASSO (3.22), (3.23) and BP (3.24), (3.25) sparse representations defined as follow:

$$= \arg \min_{\alpha} \frac{1}{2} \| \alpha - \frac{1}{T} \sum_{t=1}^T v_t \alpha_t \|^2 + \lambda \|\alpha\|_1 \quad \text{where } \alpha \in \mathbb{R}^f \quad (3.22)$$

and the Dictionary Update Equation (LASSO) defined as:

$$= \arg \min_D \frac{1}{2} \sum_{t=1}^T \| x_t - D \alpha_t \|^2 + \lambda \sum_{i=1}^f \| d_i \|^2 \quad \text{where } D \in \mathbb{C} \quad (3.23)$$

$$= \arg \min_{\alpha} \|\alpha\|_1 \quad \text{s.t. } D_{t-1} \alpha = x_t \quad \text{where } \alpha \in \mathbb{R}^f \quad (3.24)$$

and the Dictionary Update Equation (BP) defined as:

$$= \arg \min_D \frac{1}{2} \sum_{t=1}^T \| x_t - D \alpha_t \|^2 \quad \text{s.t. } \frac{1}{2} \sum_{t=1}^T \| \alpha_t \|^2 \leq \epsilon \quad \text{where } D \in \mathbb{C} \quad (3.25)$$

$$C = \{ D_i \in \mathbb{R}^{n_b \times f} \text{ s.t. } \forall j=1, \dots, f, i=0, \quad |d'_{ij}| \leq 1 \} \quad (3.26)$$

There are two algorithms in sparsity-based hyperspectral image compression work environment: dictionary learning and dictionary update. That it presented with the sparse representation equations (LASSO and BP), these equations that presented above corresponding to the numbers (3.22), (3.23), (3.24) and (3.25)

### Algorithm 1: Dictionary learning

Build random initial dictionary  $D_0$

Set  $A_0$  and  $B_0$  matrices to zero initially

for  $t = 1 : T$

Choose  $x_t \in \mathbb{R}^{n_b}$  randomly from hyperspectral data

'Equation of sparse coding' (3.22) or (3.24)  $\longrightarrow$  based on the

representation Update  $A_t = A_{t-1} + \alpha_t \alpha_t^T$  and  $B_t = B_{t-1} + x_t \alpha_t^T$

Evaluate  $D_t$  depending on Dictionary Update Algorithm

End for

Gain learned dicti

### Algorithm 2: Dictionary Update

$D_t$  is computed by utilizing  $D_{t-1}$ ,  $A_t$  and  $B_t$  in  
 “Dictionary Update Equation” ((3.23) or (3.25))

Based on the sparse representation repeat

for  $j = 1 : f$

Find  $j$ th column of  $D_t$  depending on one of equations of sparse representation

where

$D = [d_1, \dots, d_f] \in \mathbb{R}^{n_b \times f}$ ,  $A = [a_1, \dots, a_f] \in \mathbb{R}^{f \times f}$  and

$B = [b_1, \dots, b_f] \in \mathbb{R}^{n_b \times f}$  ( $U_j = 1/A_{j,j}$ ) ( $b_j = D_{aj} + d_j$ )

$d_j = 1 / \max(\|u_j\|_2, 1)$  and  $E_j = \text{sqr}(\sum_{b'} |d_j^t - d_j^{t-1}|^2)$   
 1) End for

until  $E < \text{Threshold}$

Use  $D$  in Dictionary Learning Algorithm (Ülkü, and Töreyn, 2015b)

Hence, a sparse representation is obtained for the low-band block,  $X_L$ , by an online learning based hyperspectral image compression framework. The framework consists of dictionary learning and dictionary update sub-algorithms that are applied in an alternating fashion (Ülkü, and Töreyn, 2015b). The sub-algorithms make use of different sparse coding ((3.22), (3.24)) and dictionary update equations ((3.23), (3.25)) to obtain BP or LASSO based sparse representations. Finally, the framework yields a set of sparse coefficients,  $\alpha$ , that represents the low-band block,  $X_L$ .

One may further decompose the spectral vector,  $x_{i,j}[k]$ , using successive levels of integer wavelet filters in order to obtain a smaller low-band block,  $X_L$ . In this thesis, we apply two and three levels of decomposition in order to obtain further spectral decorrelation (cf. Figure 3.3).

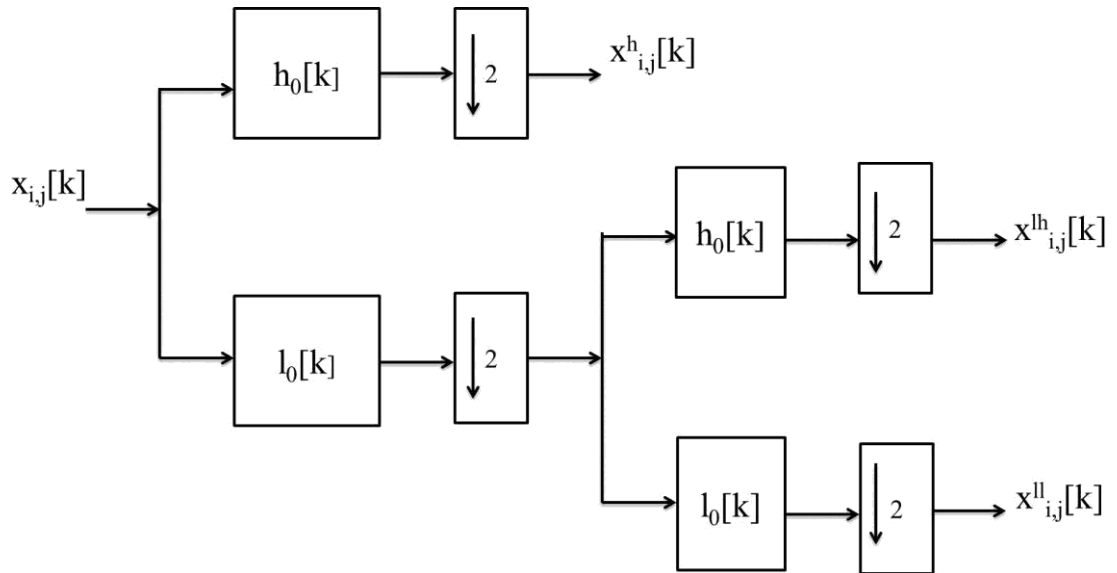


**Figure 3.3** Two-level integer wavelet transform applied to  $x_{i,j}[k]$  for further spectral decorrelation. In this thesis, upto three levels are applied.

The integer wavelet transform can be reconstructed in a perfect manner by a set of reconstruction filters,  $h_1[k]$  and  $l_1[k]$  which may be obtained as follows (Strang and Nguyen, 2011):

$$h_1[k] = (-1)^k l_0[k] \quad (3.27)$$

$$l_1[k] = (-1)^{k+1} h_0[k] \quad (2.28)$$

where  $h_1[k]$  stands for the highpass filter coefficients and  $l_1[k]$  stands for the lowpass filter coefficients in the synthesis (reconstruction) stage (cf. Figure 3.4). The synthesized (reconstructed) signal (spectral vector) is represented by  $\hat{x}_{i,j}[k]$ .

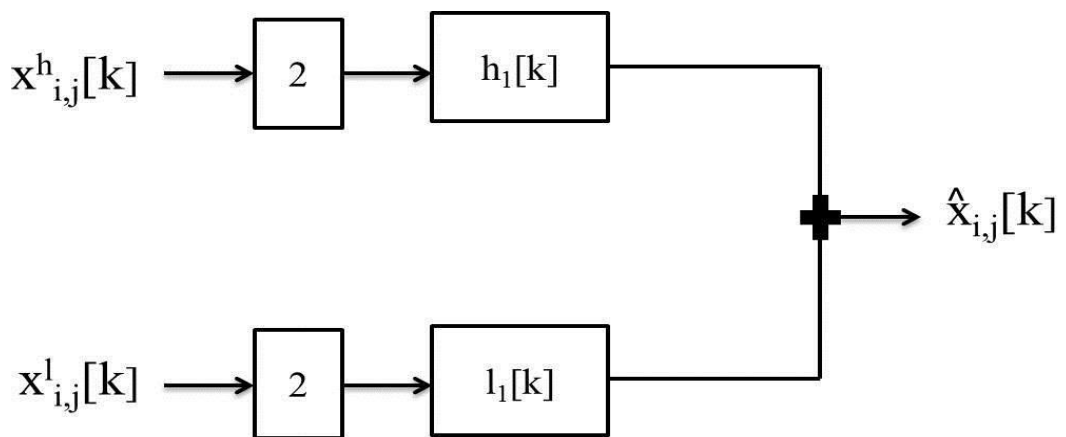


**Figure 3.4** Single-level (perfect) reconstruction stage corresponding to integer wavelet transforms.

Similar reconstruction stages may be deployed for higher (two or three) level decompositions.

Once the reconstructed spectral vector,  $\hat{x}_{ij}[k]$ , is obtained, the reconstructed data cube,  $\hat{x}$ , can be formed as follows:

$$\hat{x}_{ij}[k] = \begin{cases} \hat{x}_{ij}[k] & \text{if } k=1, \dots, n_b \\ 0 & \text{if } k=n_b+1, \dots, n_b+n_s \end{cases} \quad (3.29)$$

where  $k=1, \dots, n_b$ , at the  $(i,j)$ -th spatial location, and,  $i=1, \dots, n_i$ , and  $j=1, \dots, n_s$ .

The performance of the hybrid compression scheme is measured based on peak-signal-to-noise-ratio (PSNR):

$$\text{PSNR} = 10 \log_{10} \frac{(2^{nd})^2}{M} \quad (3.30)$$

where  $nd$  stands for the bit-depth of the values in  $X$  and  $M$  stands for the mean-square-error:

$$M = \frac{1}{\sum_{i=1}^{n_i} \sum_{j=1}^{n_s} \sum_{k=1}^{n_b} (x_{ij}[k] - \hat{x}_{ij}[k])^2} \quad (3.31)$$

It is expected to have a better PSNR performance for reconstructed data cubes,  $\hat{x}$ , that are obtained using higher level spectral decorrelations. In the following chapter, comparative compression results are presented for several methods applied on two hyperspectral images.

## 4 RESULTS AND DISCUSSIONS

### 4.1 Experimental Data Set

In here, we classify experiments that we made: we used two different test dataset hyperspectral images that have different size (Low Altitude and Erta Ale ), which was detailed in (Table 4.1). We examined with the Airborne Visible / Infrared Imaging Spectrometer (AVIRIS) and hyperion datasets (Kiely and Klimesh, 2009). In this thesis, we analyze part of the data that is cropped into a smaller cube of size 256x256x224. Comparative results are presented in the following tables for various decorrelation integer wavelet filters with varying decomposition levels, different dictionary sizes,  $f$ , and various sparse representations, such as BP and LASSO.

Table 4.1 Image Specifications of AVIRIS/HYPERION Hyperspectral Data

<b>AVIRIS HYPERSPECTRAL DATA</b>						
Name	No. Samples	No. Lines	No. Bands	Bit depth	Flight Number	year
<b>Low Altitude</b>	614	3689	224	16	f960705t01p02_r05	1996
<b>HYPERION HYPERSPECTRAL DATA</b>						
Name	No. Samples	No. Lines	No. Bands	Bit depth	image Number	year
<b>Erta Ale</b>	256	3187	242	12	EO1H1680502010057110KF	2010

Throughout the comparisons, the bit-rate,  $r$ , measured in bits-per-sample, is evaluated using the following equation:

$$r = n \frac{c2}{c1} \quad (4.1)$$

where  $nd$  is the bit-depth,  $c1$  is the size of the original data cube,  $X$ , and  $c2$  is the sum of sizes of compressed high band data, size of the number of sparse coefficients and the size of dictionary learning.

Compression performances of online sparse-coding algorithms for the processed cubes present in below tables proposed the performances of compression of online sparse-coding algorithms. As well as the compression process is presented in the tables below are for a set of filters also the two sets of data for three levels WT decomposition, which showed close results for each BPS comes a reason for the convergence of image data

values and due to we dealt with lossless approach. As we mentioned above that the compression process is performed by the values of PSNR conformity with the BPS values. In below figure (4.1) Hyperspectral data is decomposed where (a) low (L) and high (H) sub - band images by correlating it with single level, (b) (H), (LH) and (LL) for two-level and (c) (H),( LH), (LLH) and(LLH) for two level filter banks wavelet transform. For this purpose, the researcher applies the sub-samplers with the above filter banks in the (d) (x, y) position of the original data.

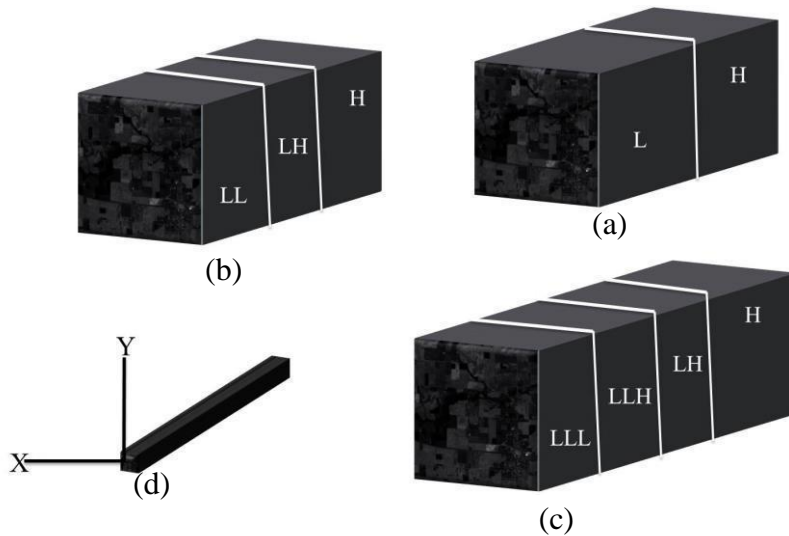


Figure 4.1. Three-level spectral decorrelation of Hyperspectral data. The data blocks named as H, LH and LLH, are all compressed using JPEG2000 – lossless mode, whereas, LLL and LL are compressed using sparse representations

In addition to that has been mentioned and detailed we will show it in the following tables are related to compression performances corresponding to the bit rate, LASSO



and BP- representation-based online sparse-coding algorithms measured by PSNR values for Low Altitude and Erta Ale datasets. Where f is the number of columns in the dictionary, BPS bit rate sample and BPSD bit rate sample with dictionary learning. In (Tables 4.2-4.25). Among the f-value-coded hyperspectral images, the best PSNR values are acquired by the data compressed using LASSO, and BP-representation-based online sparse coding algorithms for 3 levels

**Table 4.2** Haar filter bank, Low Altitude, LASSO sparse representation

f	PSNR 1- level	PSNR 2- levels	PSNR 3- levels	BPS 1- level	BPS 2- levels	BPS 3- levels	BPSD 1- level	BPSD 2- levels	BPSD 3- levels
1	0138004	4834.80	4403.401	0.1	0.1	0.1	8.1	4.1	2.1
2	4434444	4834.84	4403.10.	0.1	0.1	0.19	8.1	4.18	2.1
3	4438484	4834.8.	44030188	0.2	0.2	0.2	8.2	4.2	030
4	443.048	4834404	44030008	0.3	0.3	0.3	8.3	4.3	2.3
5	4034411	4834.88	44030888	0.3	0.3	0.4	8.3	4.39	2.4
10	40300.0	4834.10	44030844	0.7	0.7	0.7	8.7	4.7	2.7

**Table 4.3** Haar filter bank , Low Altitude, BP sparse representation

f	PSNR 1- level	PSNR 2- levels	PSNR 3- levels	BPS 1- level	BPS 2- levels	BPS 3- levels	BPSD 1- level	BPSD 2- levels	BPSD 3- levels
1	0138004	4834.80	4403.401	0.1	0.1	0.1	8.1	4.1	2.1
2	4434444	4834.84	4403.10.	0.1	0.1	0.19	8.1	4.18	2.1
3	4438484	4834.8.	44030188	0.2	0.2	0.2	8.2	4.2	030
4	443.048	4834404	44030008	0.3	0.3	0.3	8.3	4.3	2.3
5	4034411	4834.88	44030888	0.3	0.3	0.4	8.3	4.39	2.4
10	40300.0	4834.10	44030844	0.7	0.7	0.7	8.7	4.7	2.7

In the following tables, the PSNR values corresponding to different compression cases are presented. Tables (4.2) and (4.3) are corresponding to compression performance for the Haar filter bank. Similarly, consecutive tables are populated with PSNR and bit-rate values that correspond to other integer wavelet filters, such as 9/7, 9/3, 5/3, 5/11 and 2/6. Apparently, the best performance was achieved by Haar, 5/3 and 9/3 based spectral decorrelation filters.

**Table 4.4** 9/7 filter bank, Low Altitude ,LASSO sparse representation

f	PSNR -4 level	PSNR 2- levels	PSNR -. levels	BPS -4 level	BPS -0 levels	BPS -. levels	BPSD -4 level	BPSD -0 levels	BPSD -. levels
1	0.384	48308.8	.0304.8	0.1	0.1	0.1	83.	4.1	2.1
2	00340	48308.8	94.40	0.2	0.1	0.2	8.4	4.18	2.1
3	00308	48301	.03.184	0.3	0.2	0.3	8.5	4.2	2.2
4	0030.	48301	.0304	0.3	0.3	0.3	8.6	4.3	2.3
5	00300	48301	.030.	0.4	0.39	0.4	8.6	4.39	2.39
10	0034.	4830140	.0304	0.8	0.7	0.8	9	4.7	2.7

**Table 4.5** 9/7 filter bank , Low Altitude, BP sparse representation.

f	PSNR level -4	PSR -0 levels	PSNR -. levels	BPS -4 level	BPS -0 levels	BPS -. levels	BPSD -4 level	BPSD -0 levels	BPSD -. levels
1	0.311.4	48308.8	.034.10	0.1	0.1	0.1	83.	4.1	2.1
2	0034814	483004.	.0341.4	0.2	0.1	0.2	8.4	4.18	2.1
3	00348.4	4830..0	.034404	0.3	0.2	0.3	8.5	4.2	2.2
4	0034008	4830..4	..38048	0.3	0.3	0.3	8.6	4.3	2.3
5	003404.	4830.88	.03404.	0.4	0.39	0.4	8.6	4.39	2.39
10	0034408	4830.88	..3.00.	0.8	0.7	0.8	9	4.7	2.7

**Table 4.6** 5/3 filter bank, Low Altitude,LASSO sparse representation.

f	PSNR -4 level	PSNR levels -0	PSNR levels -.	BPS -4 level	BPS -0 levels	BPS -. levels	BPSD -4 level	BPSD -0 levels	BPSD -. levels
1	08341	57.0355	440314.0	0.1	0.1	0.1	8.1	4.1	2.1
2	48.03	57.0357	4403888.	0.17	0.1	0.2	8.2	034	2.2
3	08344	57.0360	44038.00	0.2	0.2	0.3	8.3	4.2	2.3
4	01384	57.0357	44038.48	0.3	0.3	0.39	8.3	03.	2.39
5	0834.	57.0354	44038.4.	0.39	0.3	0.4	8.4	03..	2.4
10	08341	4134.48	44038.41	0.7	0.7	0.8	8.8	4.7	2.8

**Table 4.7** 5/3 filter bank , Low Altitude, BP sparse representation

f	PSNR level -4	PSR -0 levels	PSNR levels -.	BPS -4 level	BPS -0 levels	BPS -. levels	BPSD -4 level	BPSD -0 levels	BPSD -. levels
1	0438008	4134.11	44034400	0.1	0.1	0.1	8.1	4.1	2.1
2	43.9039	483.8.8	44034840	0.17	0.1	0.2	8.2	034	2.2
3	0.34804	483.848	44034..4	0.2	0.2	0.3	8.3	4.2	2.3
4	003..01	483.884	44031444	0.3	0.3	0.39	8.3	03.	2.39
5	0830401	483.184	44038.01	0.39	0.3	0.4	8.4	03..	2.4
10	0834.48	4134444	44038414	0.7	0.7	0.8	8.8	4.7	2.8

**Table 4.8** 9/3 filter bank, Low Altitude, LASSO sparse representation

K.	PSNR -4 level	PSNR -0 levels	PSNR levels -. .	BPS -4 level	BPS -0 levels	BPS -. levels	BPSD -4 level	BPSD -0 levels	BPSD -. levels
1	0034.	483.80.	4403848.	0.1	0.1	434	8.2	4.1	2.1
2	04340	483.8.0	44038481	0.17	0.17	434.	8.3	4.18	2.19
3	04344	483.8	440384..	0.2	0.2	0.2	83.	4.2	030
4	0438.	483.8	440384.0	0.3	0.3	0.3	8.4	4.3	2.3
5	0438.	483.8.0	4403884.	0.39	0.39	0.4	834	4.39	2.4
10	043..	483.8.0	44038844	0.7	0.7	0.7	8.8	4.7	2.7

**Table 4.9** 9/3 filter bank, Low Altitude, BP sparse representation

K.	PSNR level -4	PSNR -0 levels	PSNR levels -. .	BPS -4 level	BPS -0 levels	BPS -. levels	BPSD -4 level	BPSD -0 levels	BPSD -. levels
1	003488.	483.80.	44034408	0.1	0.1	434	8.2	4.1	2.1
2	0438.80	4830800	44.34888	0.17	0.17	434.	8.3	4.18	2.19
3	0438404	4830844	4403.4.4	0.2	0.2	0.2	83.	4.2	030
4	04384.8	4830..8	44030104	0.3	0.3	0.3	8.4	4.3	2.3
5	0438040	4830...	44034480	0.39	0.39	0.4	834	4.39	2.4
10	0438040	48301..	4403080.	0.7	0.7	0.7	8.8	4.7	2.7

**Table 4.10** 5/11 filter bank, Low Altitude ,LASSO sparse representation

f	PSNR 1- level	PSNR -0 levels	PSNR levels -. .	BPS -4 level	BPS -0 levels	BPS -. levels	BPSD -4 level	BPSD -0 levels	BPSD -. levels
1	0030440	4834004	44034.84	0.1	0.1	0.1	8.3	4.1	2.1
2	04300.0	483400.	44034448	0.17	0.17	0.19	8.3	4.18	034.
3	043.1	4834004	44034000	0.2	0.2	0.2	8.4	4.2	2.2
4	043.0	4834000	44034004	0.3	0.3	0.3	8.5	4.3	2.3
5	043.4	4834000	44034004	0.38	0.39	0.4	8.6	4.3	2.4
10	043.0	4834000	44034004	0.7	0.7	0.7	8.6	4.7	2.7

**Table 4.11** 5/11 filter bank, Low Altitude ,BP sparse representation

f	PSNR level -4	PSNR -0 levels	PSNR levels -. .	BPS -4 level	BPS -0 levels	BPS -. levels	BPSD -4 level	BPSD -0 levels	BPSD -. levels
1	0030.80	4834040	44034448	0.1	0.1	0.1	8.3	4.1	2.1
2	043...4	4834448	4403444.	0.17	0.17	0.19	8.3	4.18	034.
3	043.4.0	443..88	44034400	0.2	0.2	0.2	8.4	4.2	2.2
4	043..0.	4834480	440344.0	0.3	0.3	0.3	8.5	4.3	2.3
5	0430444	443..81	440344.1	0.38	0.39	0.4	8.6	4.3	2.4
10	043.10.	4834441	44034441	0.7	0.7	0.7	8.6	4.7	2.7

**Table 4.12** 2/6 filter bank, Low Altitude ,LASSO sparse representation

f	PSNR -4 level	PSNR -0 levels	PSNR levels -.	BPS -4 level	BPS -0 levels	BPS -. levels	BPSD -4 level	BPSD -0 levels	BPSD -. levels
1	08388	40314..	44034148	0.1	0.1	0.1	8.1	4.1	2.1
2	08381	4031404	44034.88	0.1	0.1	0.1	8.1	4.1	2.1
3	0.340	40314..	44034444	0.2	0.2	0.2	8.3	4.2	2.2
4	0.340	40314.1	4403444.	0.3	0.3	0.3	8.3	4.3	2.3
5	083.0	40314.1	44034444	0.3	0.3	0.4	8.4	4.39	2.4
10	083.8	40314.1	4403444.	0.7	0.7	0.7	8.8	4.7	2.7

**Table 4.13** 2/6 filter bank , Low Altitude,BP sparse representation.

f	PSNR level -4	PSNR -0 levels	PSNR levels -.	BPS -4 level	BPS -0 levels	BPS -. levels	BPSD -4 level	BPSD -0 levels	BPSD -. levels
1	083881.	40314..	4443..00	0.1	0.1	0.1	8.1	4.1	2.1
2	0831844	40314.8	44034444	0.1	0.1	0.1	8.1	4.1	2.1
3	083.840	40314.8	44034484	0.2	0.2	0.2	8.3	4.2	2.2
4	0.3448.	40314..	44034.4.	0.3	0.3	0.3	8.3	4.3	2.3
5	0.34484	40314.1	44034.80	0.3	0.3	0.4	8.4	4.39	2.4
10	0.34800	40314.4	44034.04	0.7	0.7	0.7	8.8	4.7	2.7

**Table 4.14** Haar filter bank, Erta Ale, LASSO sparse representation

f	PSNR level -4	PSNR -0 levels	PSNR levels -.	BPS -4 level	BPS -0 levels	BPS -. levels	BPSD -4 level	BPSD -0 levels	BPSD -. levels
1	4.3.1	4834440	44030844	0.08	0.09	0.1	6.0	1.6	3.0
2	4034004	4834444	44034880	0.1	0.1	0.15	6.1	1.65	3.1
3	403448.	4834400	104.4745	0.19	0.19	0.2	6.19	1.7	3.19
4	4034408	4834444	44030.4.	0.2	0.2	0.26	6.2	1.76	3.2
5	4034440	4834404	440308.4	0.29	0.3	0.3	6.29	1.8	3.3
10	40344.4	4834448	44030881	0.5	0.5	0.5	6.5	2.08	3.5

**Table 4.15** Haar filter bank, Erta Ale, BP sparse representation

f	PSNR level -4	PSNR 2- levels	PSNR levels -.	BPS -4 level	BPS -0 levels	BPS -. levels	BPSD -4 level	BPSD -0 levels	BPSD -. levels
1	4.3.084	4834408	4403410.	0.2	0.2	0.3	6.2	3.2	1.8
2	4.3.444	483444.	44030444	0.29	0.29	0.4	6.2	3.2	1.9
3	4.3.8.4	4834408	44030.01	0.3	0.3	0.47	6.3	3.3	1.97
4	403484.	4834001	4403..14	0.4	0.4	4340	6.4	3.4	2.0
5	4.3.8.0	483440.	44030800	0.4	0.4	0.58	6.4	3.4	2.0
10	4434004	4834084	44030188	0.5	0.7	0.8	6.7	3.7	2.3

**Table 4.16** 9/7 filter bank , Erta Ale, LASSO sparse representation

K.	PSNR level -4	PSNR -0 levels	PSNR -. levels	BPS -4 level	BPS -0 levels	BPS -. levels	BPSD -4 level	BPSD -0 levels	BPSD -. levels
1	4030418	4830488	.03414.	0.1	0.09	0.1	6.1	3.0	1.6
2	4030404	4830488	.0340.1	0.2	0.1	0.2	6.2	3.1	1.7
3	4030410	483048.	.034..4	0.2	0.19	0.26	6.2	3.1	1.7
4	4030414	4830488	.034.14	0.3	0.2	0.3	6.3	3.2	1.8
5	4030440	4830488	.034884	0.36	0.3	0.37	6.36	3.3	1.87
10	4030404	4830481	.0304	0.6	0.5	0.6	6.6	3.5	2.1

**Table 4.17** 9\7 filter bank, Erta Ale, BP sparse representation

K	PSNR level -4	PSNR -0 levels	PSNR -. levels	BPS -4 level	BPS -0 levels	BPS -. levels	BPSD -4 level	BPSD -0 levels	BPSD -. levels
1	4034844	4830488	.030841	0.1	0.1	0.4	3.1	3.1	3.4
2	4030404	483..11	.034080	0.2	0.2	0.5	3.2	3.2	3.5
3	4030410	483.8..	.030080	0.2	0.2	0.5	3.2	3.2	3.5
4	4030414	483.881	.0340.0	0.3	0.3	0.6	3.3	3.3	3.6
5	4030440	483.888	.034481	0.36	0.3	0.69	3.3	3.3	3.69
10	4030404	483.8.4	.034141	0.6	0.6	0.9	3.6	3.6	3.9

**Table 4.18** 5\3 filter bank , Erta Ale, LASSO sparse representation

K.	PSNR 1-level	PSNR 2- levels	PSNR 3-levels	BPS -4 level	BPS -0 levels	BPS -. levels	BPSD -4 level	BPSD -0 levels	BPSD -. levels
1	4034.48	41344.8	44034084	0.09	0.09	0.1	6.0	3.0	1.6
2	4034800	41344..	44034.88	0.1	0.1	0.2	6.1	3.1	1.7
3	403410.	57.0360	44034.08	0.19	0.19	0.2	6.19	3.1	1.7
4	4034141	4134844	44034.80	0.2	0.2	0.3	6.2	3.2	1.8
5	4034100	4134840	44034.44	0.3	0.3	0.36	6.3	3.3	1.87
10	40348.0	41344..	44034.80	0.5	0.5	0.6	6.5	3.5	2.1

**Table 4.19** 5\3 filter bank, Erta Ale, BP sparse representation

K.	PSNR 1- level	PSNR 2- levels	PSNR 3-levels	BPS -4 level	BPS -0 levels	BPS -. levels	BPSD -4 level	BPSD -0 levels	BPSD -. levels
1	4.3.884	4134844	4403.840	0.2	0.2	0.3	6.2	3.2	1.8
2	4034088	4134400	44034440	0.3	0.3	0.39	6.3	3.3	1.89
3	4034.40	41344..	44034011	0.3	0.38	0.4	6.3	3.3	1.9
4	4034.88	4134040	440348.4	0.4	0.4	.5	6.4	3.4	2.0
5	403444.	41344.8	44038084	0.49	0.49	.5	6.49	3.49	2.0
10	40341.4	4134444	44034018	0.7	0.7	0.8	6.7	3.7	2.3

**Table 4.20** 9\3 filter bank, Erta Ale, LASSO sparse representation

K.	PSNR level -4	PSNR 2- levels	PSNR levels -.	BPS -4 level	BPS -0 levels	BPS -. levels	BPSD -4 level	BPSD -0 levels	BPSD -. levels
1	4034401	483..00	44034401	0.09	0.09	0.1	6.0	3.0	1.6
2	4034484	483..01	44034444	0.1	0.1	0.1	6.1	3.1	1.65
3	4034400	483..08	44034444.	0.19	0.19	0.19	6.19	3.1	1.7
4	4034480	483..80	44034444.	0.2	0.2	0.2	6.2	3.2	1.76
5	4034401	483..08	44034484	0.3	0.3	0.3	6.3	3.3	1.8
10	4034411	56.3950	44034444.	0.5	0.5	0.5	6.5	3.5	2.08

**Table 4.21** 9\3 filter bank, Erta Ale, BP sparse representation

K.	PSNR level -4	PSNR -0 levels	PSNR levels -.	BPS -4 level	BPS -0 levels	BPS -. levels	BPSD -4 level	BPSD -0 levels	BPSD -. levels
1	40344.8	483..04	4403.0.0	0.2	0.2	0.3	6.2	3.2	1.8
2	4034040	483.48.	44034.44	0.3	0.3	0.4	6.3	3.3	1.9
3	4034008	4830.04	44030401	0.38	0.38	0.47	6.3	3.3	1.97
4	4034084	483.441	44034441	0.4	0.4	4340	6.4	3.4	2.0
5	4034144	4830.04	44034..8	0.49	0.49	0.58	6.49	3.49	2.0
10	4034411	56.3006	44030004	0.7	0.7	0.8	6.7	3.7	2.3

**Table 4.22** 11\5 filter bank, Erta Ale, LASSO sparse representation

K.	PSNR level -4	PSNR 2- levels	PSNR levels -.	BPS -4 level	BPS -0 levels	BPS -. levels	BPSD -4 level	BPSD -0 levels	BPSD -. levels
1	40300.4	4834004	4403...4	0.08	0.1	0.1	6.0	3.0	1.6
2	40300..	4834000	4403.184	0.1	0.1	0.1	6.1	3.1	1.65
3	40300.0	4834000	4403.818	0.19	0.19	0.19	6.19	3.1	1.7
4	4030484	4834000	4403.814	0.2	0.2	0.2	6.2	3.2	1.76
5	40300..	4834044	4403.814	0.29	0.3	0.3	6.3	3.3	1.8
10	40300.0	4834014	4403.880	0.5	0.5	0.5	6.5	3.5	2.08

**Table 4.23** 11\5 filter bank, Erta Ale, BP sparse representation

K.	PSNR 1- level	PSNR -0 levels	PSNR levels -.	BPS -4 level	BPS -0 levels	BPS -. levels	BPSD -4 level	BPSD -0 levels	BPSD -. levels
1	40300.0	483404.	4403...8	0.09	0.1	0.1	6.0	3.1	1.6
2	40304.0	48344.4	4403.118	0.1	0.1	0.2	6.1	3.1	1.7
3	4030480	483440.	4403.810	0.2	0.2	0.2	6.2	3.2	1.7
4	403048.	48344.4	4403.81.	0.25	0.2	0.3	6.2	3.2	1.8
5	4030844	4834400	4403.881	0.3	0.3	0.3	6.3	3.3	1.8
10	40304.1	4834484	4403.81.	0.5	0.5	0.6	6.5	3.5	2.1

**Table 4.24** 2\6 filter bank, Erta Ale, LASSO sparse representation

K.	PSNR level -4	PSNR -0 levels	PSNR levels -.	BPS -4 level	BPS -0 levels	BPS -. levels	BPSD -4 level	BPSD -0 levels	BPSD -. levels
1	403010.	4038080	44034048	0.08	0.1	0.09	6.0	3.0	1.6
2	40301.4	4038080	4403404.	0.1	0.1	0.1	6.1	3.1	1.65
3	403010.	4038081	44034048	0.19	0.19	0.19	6.19	3.1	1.7
4	40301.0	4038081	44034084	0.2	0.2	0.2	6.2	3.2	1.76
5	403010.	403808.	44034084	0.29	0.3	0.3	6.3	3.3	1.8
10	4030104	4038010	44034041	0.5	0.5	0.5	6.5	3.5	2.08

**Table 4.25** 2\6 filter bank, Erta Ale, BP Sparse Representations

K.	PSNR 1- level	PSNR -0 levels	PSNR levels -.	BPS -4 level	BPS -0 levels	BPS -. levels	BPSD -4 level	BPSD -0 levels	BPSD -. levels
1	4030101	4038080	44034044	0.09	0.1	0.1	6.0	3.0	1.6
2	4030188	4038084	44034018	0.1	0.1	0.1	6.1	3.1	1.65
3	4030848	40380.4	44034.48	0.19	0.2	0.2	6.19	3.1	1.7
4	4030800	40380.4	44034.48	0.2	0.2	0.2	6.2	3.2	1.76
5	4030801	40380.0	44034.00	0.3	0.3	0.3	6.3	3.3	1.8
10	40308.4	40380.0	44034.40	0.5	0.5	0.5	6.5	3.5	2.08

Results presented in tables suggest the following remarks. In BPSD which meaning of Bit Per Sample of Dictionary, have been effected gradually by f value. However, in above tables the BPSD-D1 treatments are significantly increased by raise of K values and the one dimension type is coming from size of cubes, size of alpha values and size of data after compression process (JPEG2000) continuously with depth of data. Moreover, the depth of data set are differences from data set to each other as well as shows in (Table 4.1).

The single-level decorrelation that contains 112 bands processed in a lossless manner (JPEG2000), and the remaining 112 bands are utilized to obtain a dictionary learning based sparse representation which itself is a lossy compression approach. The second type 2-level contains 168 bands of lossless (JPEG 2000) and 56 bands of dictionary learning .but the difference between 1- level and 2- levels it's not that much, the only thing is the 1- level is less than 2- levels in few points. The last one 3- levels contains 196 bands of lossless (JPEG 2000) and 28 bands of dictionary learning, the difference between 3- levels and the two other 1- level and 2- levels is higher than the difference between the first two in height points.

Results suggest that independent of filter and sparse representation type, PSNR values increase as the bit-rate value increase. Moreover, as the number of spectral decorrelation levels increase, the PSNR values also increase. This is due to the fact, as the decorrelation is carried out further, the amount of data that is compressed in a lossless manner, increases. This, in turn, affects positively the reconstructed data quality. In addition, the size of lossless compressed data block gets larger as spectral decorrelation is further carried out for more than a single-level.

Another important observation, related to the bps values is that, once the dictionary is also taken into consideration for evaluating the bit-rate, the overall bit-rate is increased by including the size of the dictionary.

#### **4.2 Rate-Distortion Comparison Results**

The rate–distortion performance of the suggested hyperspectral compression approach depend on sparse coding with online learning is gained utilizing experience data mentioned in Table 4.1.

Examine the performance of the rate-distortion Compression for each dataset and for each sparse representation (LASSO and BP).

Figures between 4.2 and 4.7 give rate-distortion performance of sparse-coding-based hyperspectral image compression ways are described for a datasets (Low Altitude and Erta ale) for the size 256x256x224. Where the PSNR measured by a logarithmic unit called decibel (dB) and bit rate by bit per sample (bps).



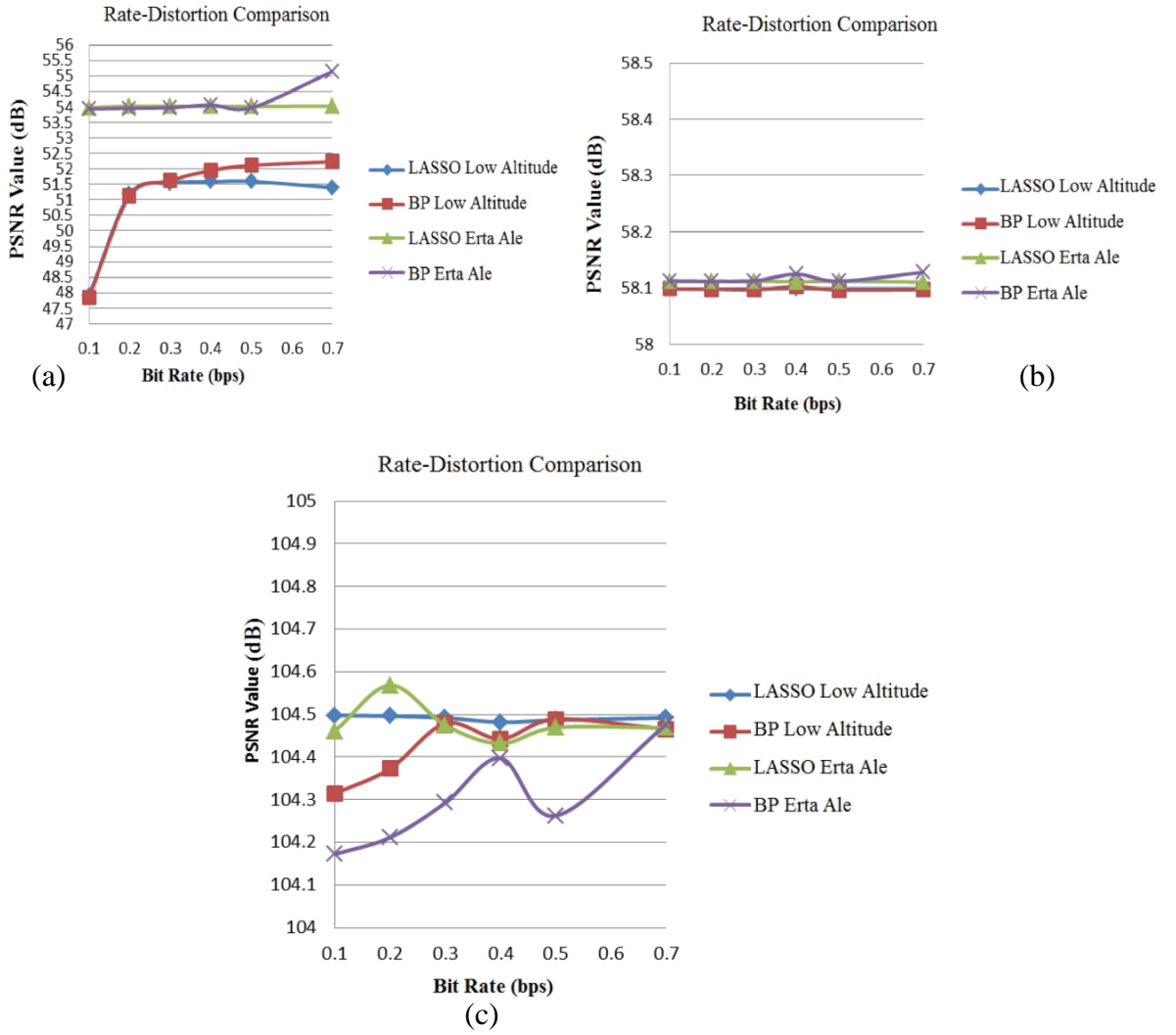
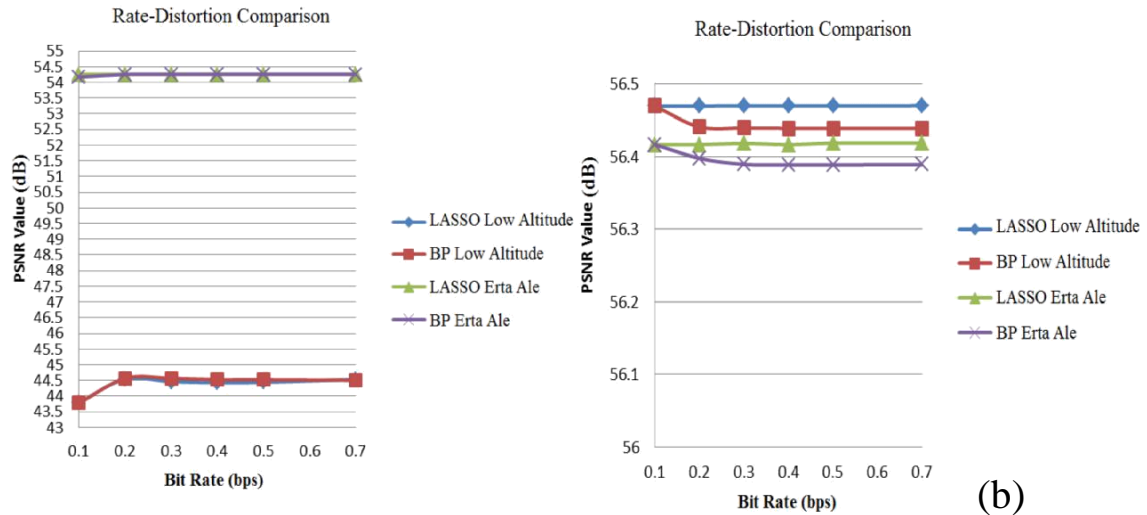
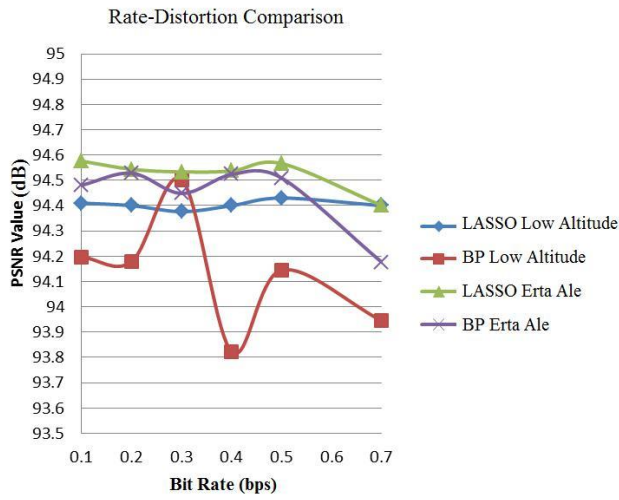


**Figure 4.2** Performance comparison of online-learning-based hyperspectral image-compression algorithms with LASSO and BP sparse representation for Low Altitude and Erta Ale are cropped as 256 lines by 256 samples by 242 bands. Using Haar filter bank (a) single level , (b) 2-level, (c) 3-level decomposition.



(a)

(b)



(c)

**Figure 4.3** Performance comparison of online-learning-based hyperspectral image compression algorithms with LASSO and BP sparse representation for Low Altitude and Erta Ale are cropped as 256 lines by 256 samples by 242 bands. Using 9/7 filter bank (a) single level, (b) 2-level, (c) 3-level decomposition.

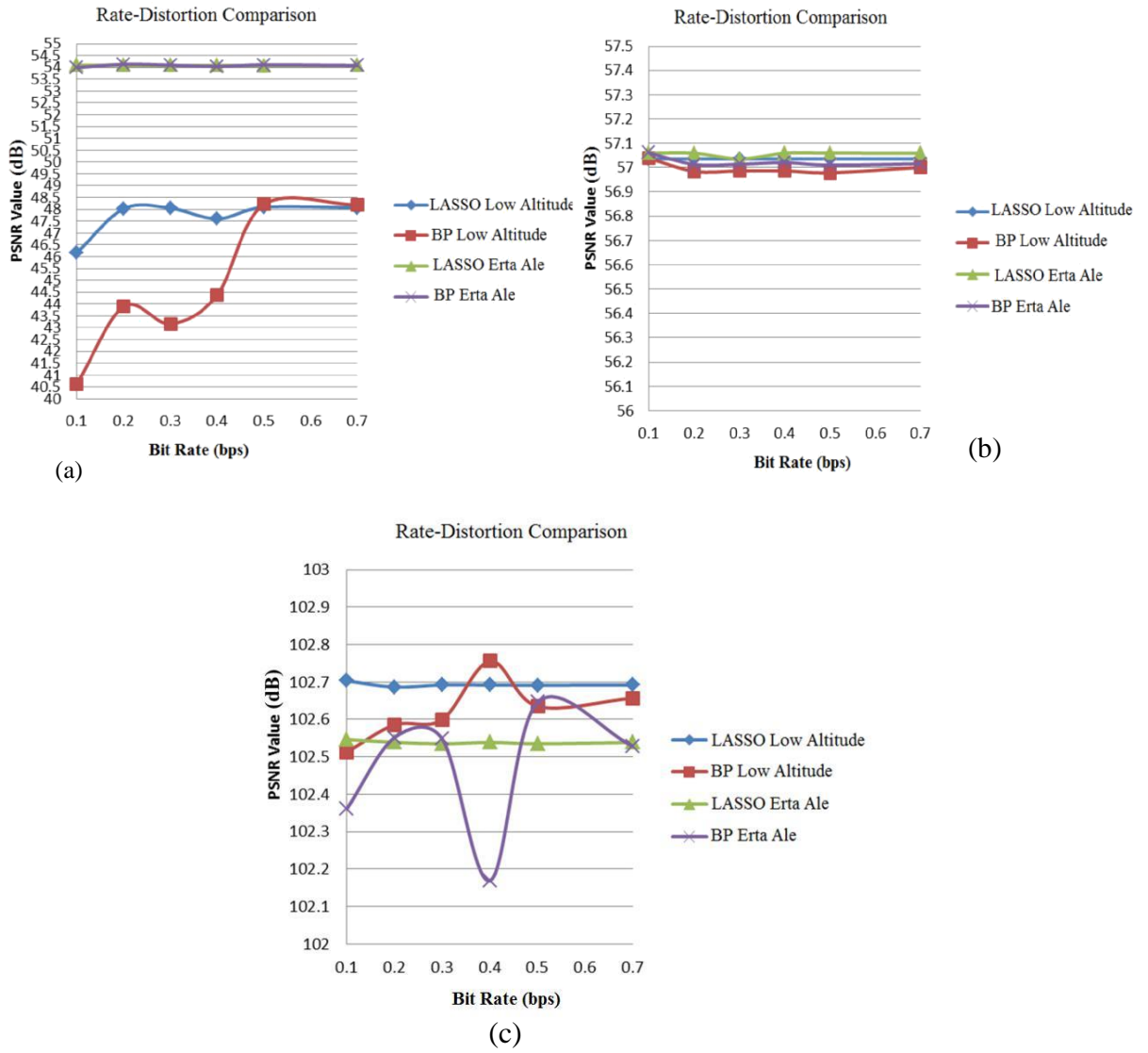


**Figure 4.4** Performance comparison of online-learning-based hyperspectral image-compression algorithms with LASSO and BP sparse representation for Low Altitude and Erta Ale are cropped as 256 lines by 256 samples by 242 bands. Using 5/3 filter bank (a) single level, (b) 2-level, (c) 3-level decomposition.

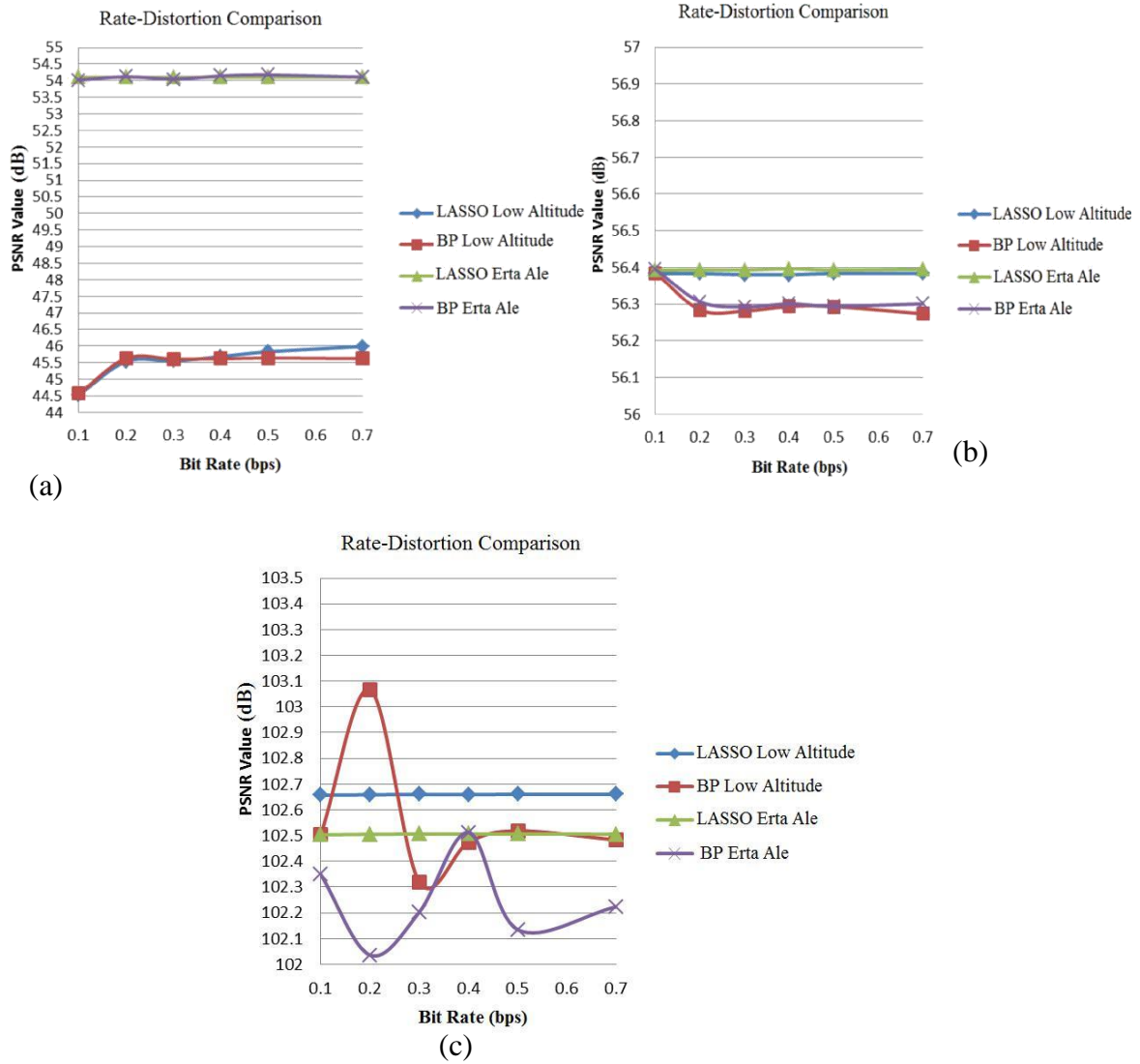


**Figure 4.5** Performance comparison of online-learning-based hyperspectral image-compression algorithms with LASSO and BP sparse representation for Low Altitude and Erta Ale are cropped as 256 lines by 256 samples by 242 bands. Using 9/3 filter bank (a) single level , (b) 2-level, (c) 3-level decomposition.

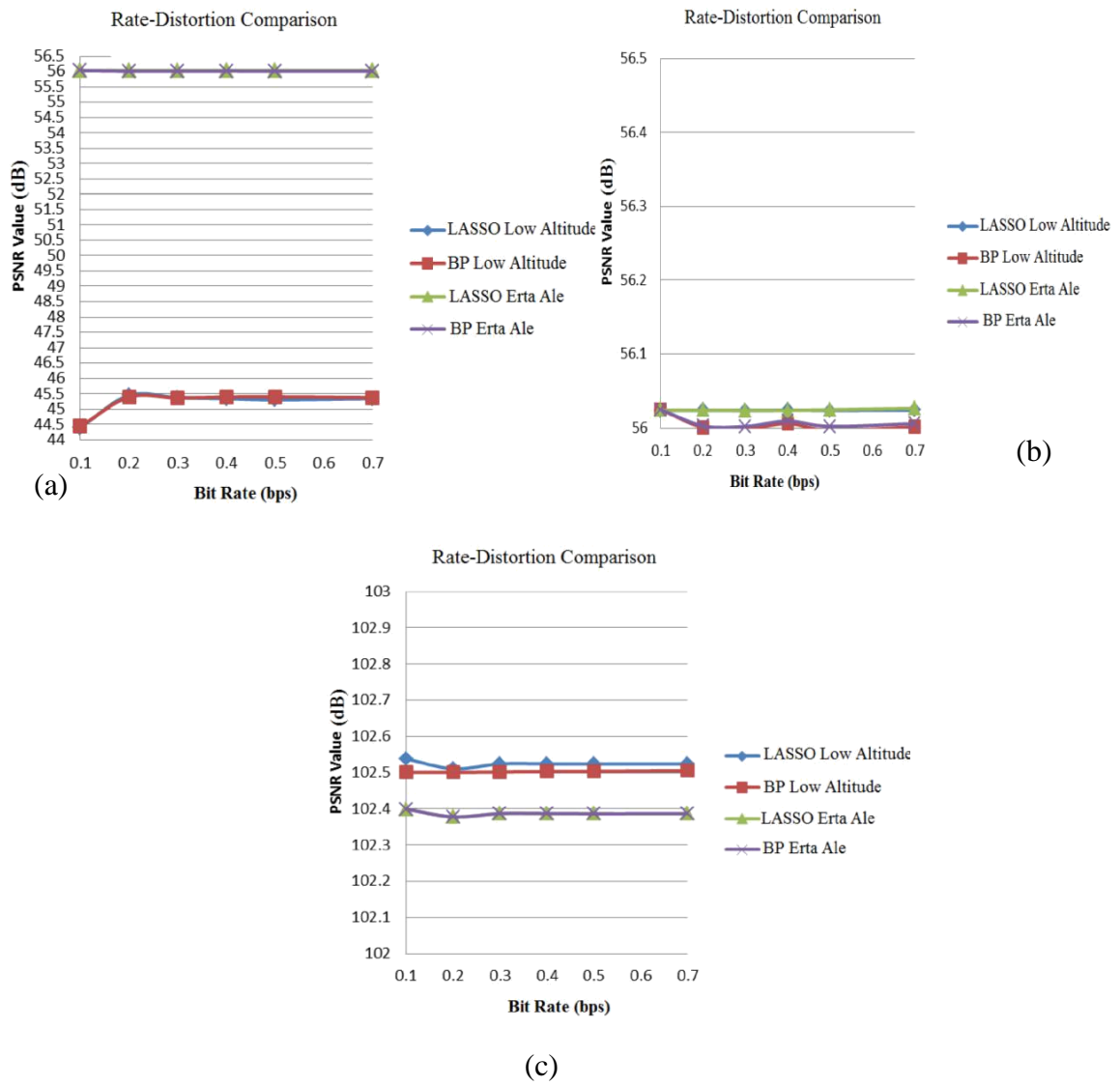


**Figure 4.6** Performance comparison of online-learning-based hyperspectral image- compression algorithms with LASSO and BP sparse representation for Low Altitude and Erta Ale are cropped as 256 lines by 256 samples by 242 bands. Using 5/11 filter bank (a) single level , (b) 2-level, (c) 3-level decomposition.

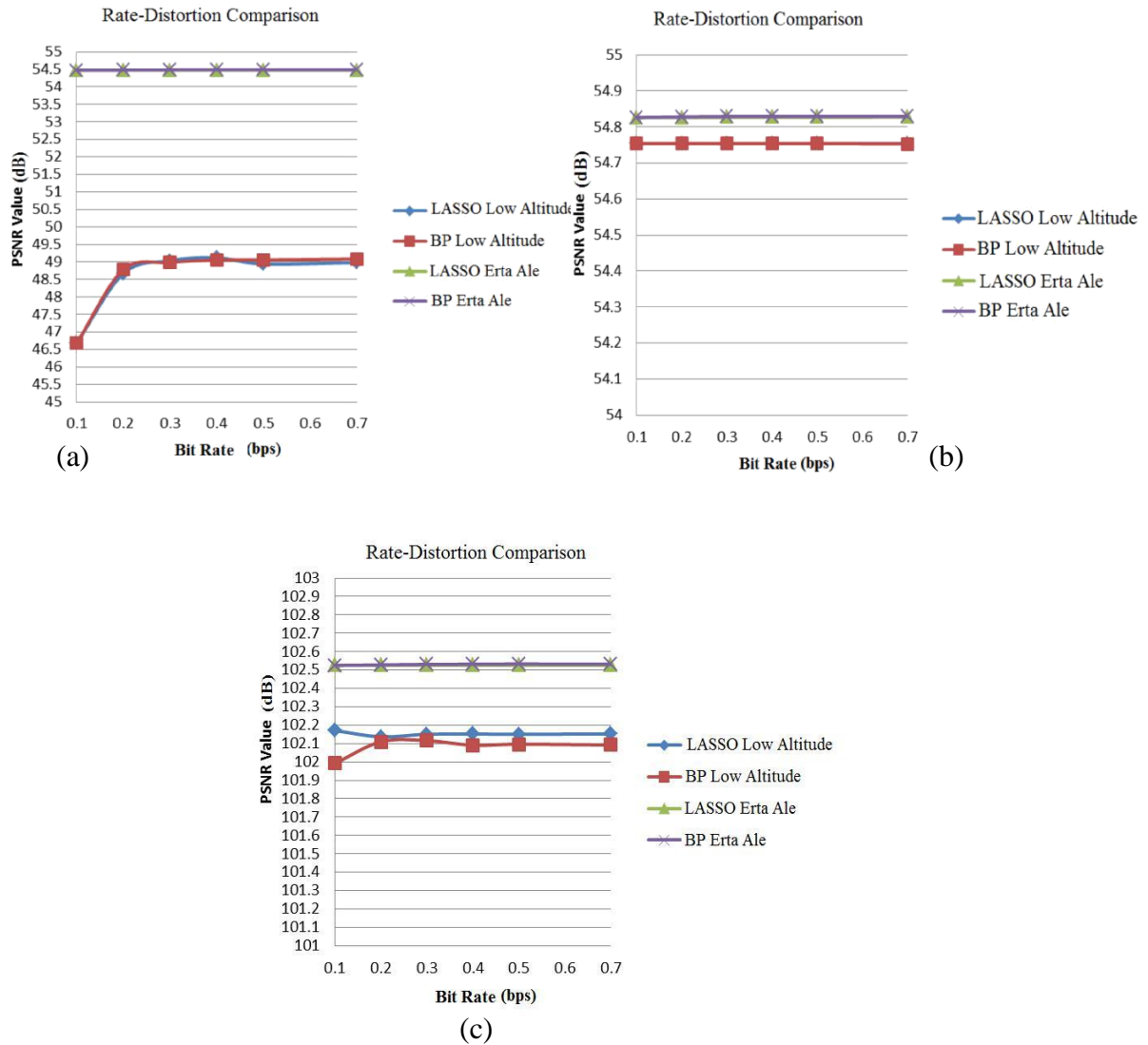


**Figure 4.7** Performance comparison of online-learning-based hyperspectral image-compression algorithms with LASSO and BP sparse representation for Low Altitude and Erta Ale are cropped as 256 lines by 256 samples by 242 bands. Using 2/6 filter bank (a) single level , (b) 2-level, (c) 3-level decomposition.

Based on the performance comparison results pertaining to the usage of different spectral decorrelation integer wavelet filters, various sparse representations and different hyperspectral data, the following conclusions may be drawn:

- As a sparse representation method LASSO performs slightly better than BP to represent the low-band block.
- There is a drastic improvement in PSNR values, once the third level for spectral decorrelation is carried out.
- The choice of spectral decorrelation integer wavelet filter does not have a strong effect on the PSNR vs. bit-rate performance.

These conclusions suggest that, a spectral decorrelation step with more than one-levels would be of paramount importance for the overall compression performance of the proposed method. Moreover, filter and sparse representation choice has a minor effect on the compression performance.





## 5 CONCLUSION AND RECOMMENDATIONS

For the lossy compression of hyperspectral data, the key aim of our research is to work into the area of sparse representation. In order that lossy compression of hyperspectral data, a modern method has been proposed for uncommon compression of data that is correlated with three levels filter banks wavelet transformation. The method depends on decompressing the data divided into two untangle sub-band image sets, the low sub-band image decomposition, and the lossless JPEG2000-based decomposition of the high sub-band. The first testing in this work has done on two the data in the AVIRIS and HYPERION hyperspectral datasets in comparison with the on top of performance hyperspectral compression ways in the literature. Which obtain infinity for the PSNR values. In addition to that by using same datasets an online-learning-based hyperspectral image compression framework is proposed. Who passed an important phases, the first phase before the update, or as it is called Dictionary Learning, the second stage is the stage of modernization. In the first transaction was obtained on the equations used, which have been preserved even in the second phase. This means relied on the representation in the process of modernization in the above stage. As well as the Bear-bit Sample calculation based on the size of the dictionary gives this hint is clear from safety process if it was send and receive dictionary learn. Also because of the difference between pixel values in spectral images, multiple types of image conversions were treated to obtain convergent values in order to reduce execution time and to obtain the most accurate results. Which are possible to be an important future work.

If we notice in the above tables (4.2 to 4.25) there is a small difference between 1-level and 2- levels, because the lossless compressing of data performed on 112 bands, while 112 was entered on the dictionary learning which consider lossy approach. In 2-levels 168 bands were subjected to lossless compression and 56 others for lossy dictionary learning. Unlike 3- levels which gave great value in all tables, this is due mostly to (Low Altitude and Erta Ale) data adopted on lossless compression (196 bands), while only 28 bands learned with dictionary learning (lossy mode).

As In our future work we try to use the above with a larger data set as well as color to get results and improve the results above, because it is possible to rely on the colors images to get the best results.

Outcomes propose that separate of the filter and sparse representation kind, PSNR values rise as the bit-rate value increase. furthermore, as the number of spectral decorrelation levels increases, the values of PSNR also raise. This is return to the reality, as the decorrelation is carried out further, the size of data that is compressed in a lossless mode, increases. This, in its role, impacts positively the reconstructed data quality. In addition, the size of lossless compressed data block gains larger as spectral decorrelation is further carried out for more than a single-level.

Also taken into account to, regarding the bps values is that, once the dictionary is also in mind into account for estimating the bit-rate, the comprehensive bit-rate is increased by including the size of the dictionary.

Based on the performance comparison outcomes respecting to the utilize of various spectral decorrelation integer wavelet filters, several sparse representations and diverse hyperspectral data, can be resulting some points, LASSO sparse representations perform best than BP to implement in the low-band block, there is a good progress in PSNR values, once the third level for spectral decorrelation is implemented.

In addition, the framework might be prolonged to include another sparse representations. moreover, search on this expansion may command to bestead compression achievement for higher bit rates.

In each of the foregoing conclusions propose that a spectral decorrelation stage with more than one levels would be of essential significance for the overall compression performance of the suggested approach.

It is possible to dive for future work by dealing with the spectral images and sparse representation rather than the dictionary learning can use neural sparse coding or K-SVD for extraction the largest possible number of transactions and use it before the update process.

## References

- Acito, N., Diani, M. and Corsini, G.,** (2011). Signal-dependent noise modeling and model parameter estimation in hyperspectral images. *IEEE Transactions on Geoscience and Remote Sensing*, 49(8), pp.2957-2971.
- Aharon, M., Elad, M. and Bruckstein, A.,** (2006).  $\ell_1$ -SVD: An algorithm for designing overcomplete dictionaries for sparse representation. *IEEE Transactions on signal processing*, 54(11), pp.4311-4322.
- Aiazzi, B., Alba, P., Alparone, L. and Baronti, S.,** (1999). Lossless compression of multi/hyper-spectral imagery based on a 3-levels fuzzy prediction. *IEEE Transactions on Geoscience and Remote Sensing*, 37(5), pp.2287-2294.
- Alaydm, J.G. and Töreyn, B.U.,** (2016), May. Sparse coding based compression of spectrally uncorrelated hyperspectral data using Haar wavelet transform. In *Signal Processing and Communication Application Conference (SIU)*, 2016 24th (pp. 1945-1948). IEEE.
- Atkinson, I., Kamalabadi, F. and Jones, D.L.,** (2003), July. Wavelet-based hyperspectral image estimation. In *Geoscience and Remote Sensing Symposium, 2003. IGARSS'03. Proceedings. 2003 IEEE International (Vol. 2, pp. 743-745)*. IEEE.
- Bahrampour, S., Nasrabadi, N.M., Ray, A. and Jenkins, W.K.,** (2016). Multimodal task-driven dictionary learning for image classification. *IEEE Transactions on Image Processing*, 25(1), pp.24-38.
- Bao, C., Ji, H., Quan, Y. and Shen, Z.,** (2016). Dictionary learning for sparse coding: Algorithms and convergence analysis. *IEEE transactions on pattern analysis and machine intelligence*, 38(7), pp.1356-1369.
- Barni, M., Papini, D., Abrardo, A. and Magli, E.,** (2005), July. Distributed source coding of hyperspectral images. In *Geoscience and Remote Sensing Symposium, 2005. IGARSS'05. Proceedings. 2005 IEEE International (Vol. 1, pp. 4-pp)*. IEEE.
- Bertsekas, D.P.,** (1999). *Nonlinear programming* (pp. 1-60). Belmont: Athena scientific.
- Bilgin, A., Zweig, G. and Marcellin, M.W.,** 2000. Three-dimensional image compression with integer wavelet transforms. *Applied optics*, 39(11), pp.1799-1814.
- Bousquet, O. and Bottou, L.,** (2008). The tradeoffs of large scale learning. In *Advances in neural information processing systems* (pp. 161-168).
- Bryt, O. and Elad, M.,** (2008). Compression of facial images using the K-SVD algorithm. *Journal of Visual Communication and Image Representation*, 19(4), pp.270-282.
- Buades, A., Coll, B. and Morel, J.M.,** (2005), June. A non-local algorithm for image denoising. In *Computer Vision and Pattern Recognition, 2005. CVPR 2005. IEEE Computer Society Conference on (Vol. 2, pp. 60-65)*. IEEE.

- Candes, E.J., Eldar, Y.C., Needell, D. and Randall, P.,** (2011). Compressed sensing with coherent and redundant dictionaries. *Applied and Computational Harmonic Analysis*, 31(1), pp.59-73.
- Charles, A.S., Olshausen, B.A. and Rozell, C.J.,** (2011). Learning sparse codes for hyperspectral imagery. *IEEE Journal of Selected Topics in Signal Processing*, 5(5), pp.963-978.
- Chen, G. and Qian, S.E.,** (2009). Denoising and dimensionality reduction of hyperspectral imagery using wavelet packets, neighbour shrinking and principal component analysis. *International Journal of Remote Sensing*, 30(18), pp.4889-4895.
- Chen, G. and Qian, S.E.,** (2011). Denoising of hyperspectral imagery using principal component analysis and wavelet shrinkage. *IEEE Transactions on Geoscience and remote sensing*, 49(3), pp.973-980.
- Chen, S.S., Donoho, D.L. and Saunders, M.A.,** (2001). Atomic decomposition by basis pursuit. *SIAM review*, 43(1), pp.129-159.
- Cheng, H., Liu, Z., Yang, L. and Chen, X.,** (2013). Sparse representation and learning in visual recognition: Theory and applications. *Signal Processing*, 93(6), pp.1408-1425.
- Cheng, K.J. and Dill, J.,** (2014). Lossless to lossy dual-tree BEZW compression for hyperspectral images. *IEEE transactions on geoscience and remote sensing*, 52(9), pp.5765-5770.
- Cheung, N.M. and Ortega, A.,** (2009). Distributed compression of hyperspectral imagery. *Distributed Source Coding*, pp.269-292.
- Christophe, E.,** (2011). Hyperspectral data compression tradeoff. In *Optical Remote Sensing* (pp. 9-29). Springer Berlin Heidelberg.
- Christophe, E., Léger, D. and Mailhes, C.,** (2005). Quality criteria benchmark for hyperspectral imagery. *IEEE Transactions on Geoscience and Remote Sensing*, 43(9), pp.2103-2114.
- Christophe, E., Mailhes, C. and Duhamel, P.,** (2008). Hyperspectral image compression: adapting SPIHT and EZW to anisotropic 3- levels wavelet coding. *IEEE Transactions on Image processing*, 17(12), pp.2334-2346.
- Christopoulos, C., Skodras, A. and Ebrahimi, T.,** (2000). The JPEG2000 still image coding system: an overview. *IEEE transactions on consumer electronics*, 46(4), pp.1103-1127.
- Chrysafis, C.G. and Ortega, A.,** (2000), December. Minimum memory implementations of the lifting scheme. In *International Symposium on Optical Science and Technology* (pp. 313-324). International Society for Optics and Photonics.
- Chui, C. J., Spring, and L. Zhong,** (1998), March. Integer Wavelet Transforms. Tech. Rep. ISO/IEC JTC/SC29/WG1 N769 Document, Geneva, Teralogic Inc.
- Conoscenti, M., Coppola, R. and Magli, E.,** (2016). Constant SNR, rate control, and entropy coding for predictive lossy hyperspectral image compression. *IEEE Transactions on Geoscience and Remote Sensing*, 54(12), pp.7431-7441.
- Dabov, K., Foi, A., Katkovnik, V. and Egiazarian, K.,** (2007). Image denoising by sparse 3- levels transform-domain collaborative filtering. *IEEE Transactions on image processing*, 16(8), pp.2080-2095.
- Davis, G.M., Mallat, S.G. and Zhang, Z.,** (1994). Adaptive time-frequency decompositions. *Optical engineering*, 33(7), pp.2183-2191.

- Dong, W., Zhang, L., Shi, G. and Li, X.,** (2013). Nonlocally centralized sparse representation for image restoration. *IEEE Transactions on Image Processing*, 22(4), pp.1620-1630.
- Dragotti, P.L., Poggi, G. and Ragozini, A.R.,** (2000). Compression of multispectral images by three-dimensional SPIHT algorithm. *IEEE Transactions on Geoscience and Remote Sensing*, 38(1), pp.416-428.
- Eismann, M.T.,** (2012), April. Hyperspectral remote sensing. Bellingham: SPIE.
- Elad, M. and Aharon, M.,** (2006). Image denoising via sparse and redundant representations over learned dictionaries. *IEEE Transactions on Image processing*, 15(12), pp.3736-3745.
- Elad, M., Figueiredo, M.A. and Ma, Y.,** (2010). On the role of sparse and redundant representations in image processing. *Proceedings of the IEEE*, 98(6), pp.972-982.
- Eldar, Y.C., Kuppinger, P. and Bolcskei, H.,** (2010). Block-sparse signals: Uncertainty relations and efficient recovery. *IEEE Transactions on Signal Processing*, 58(6), pp.3042-3054.
- Fang, L., Li, S., Duan, W., Ren, J. and Benediktsson, J.A.,** (2015). Classification of hyperspectral images by exploiting spectral-spatial information of superpixel via multiple kernels. *IEEE Transactions on Geoscience and Remote Sensing*, 53(12), pp.6663-6674.
- Friedman, J., Hastie, T. and Tibshirani, R.,** (2010). Regularization paths for generalized linear models via coordinate descent. *Journal of statistical software*, 33(1), p.1.
- Fu, W., Li, S., Fang, L., Kang, X. and Benediktsson, J.A.,** (2016). Hyperspectral image classification via shape-adaptive joint sparse representation. *IEEE Journal of Selected Topics in Applied Earth Observations and Remote Sensing*, 9(2), pp.556-567.
- Galli, L. and Salzo, S.,** (2004), September. Lossless hyperspectral compression using KLT. In *Geoscience and Remote Sensing Symposium, 2004. IGARSS'04. Proceedings. 2004 IEEE International (Vol. 1)*. IEEE.
- Goetz, A.F.,** (2009). Three decades of hyperspectral remote sensing of the Earth: A personal view. *Remote Sensing of Environment*, 113, pp.S5-S16.
- Guo, X., Huang, X., Zhang, L. and Zhang, L.,** (2013). Hyperspectral image noise reduction based on rank-1 tensor decomposition. *ISPRS journal of photogrammetry and remote sensing*, 83, pp.50-63.
- Hassanzadeh, S. and Karami, A.,** (2016). Compression and noise reduction of hyperspectral images using non-negative tensor decomposition and compressed sensing. *European Journal of Remote Sensing*, 49(1), pp.587-598.
- He, R., Zheng, W.S., Hu, B.G. and Kong, X.W.,** (2013). Two-stage nonnegative sparse representation for large-scale face recognition. *IEEE transactions on neural networks and learning systems*, 24(1), pp.35-46.
- Huang, B., Huang, H.L.A., Ahuja, A., Schmit, T.J. and Heymann, R.W.,** (2004), October. Lossless data compression for infrared hyperspectral sounders: an update. In *Optical Science and Technology, the SPIE 49th Annual Meeting (pp. 109-119)*. International Society for Optics and Photonics.

- Huo, C., Zhang, R., Yin, D., Wu, Q. and Xu, D.,** (2012), June. Hyperspectral data compression using sparse representation. In *Hyperspectral Image and Signal Processing (WHISPERS), 2012 4th Workshop on* (pp. 1-4). IEEE.
- Jin, W., Xiao-ling, Z., Lan-sun, S. and Yan, C.,** (2005), October. Hyperspectral image lossless compression using wavelet transforms and trellis coded quantization. In *Communications and Information Technology, 2005. ISCIT 2005. IEEE International Symposium on* (Vol. 2, pp. 1452-1455). IEEE.
- Karami, A., Heylen, R. and Scheunders, P.,** (2016). Hyperspectral Image Compression Optimized for Spectral Unmixing. *IEEE Transactions on Geoscience and Remote Sensing*, 54(10), pp.5884-5894.
- Karami, A., Yazdi, M. and Asli, A.Z.,** (2010), July. Hyperspectral image compression based on tucker decomposition and discrete cosine transform. In *Image Processing Theory Tools and Applications (IPTA), 2010 2nd International Conference on* (pp. 122-125). IEEE.
- Karami, A., Yazdi, M. and Asli, A.Z.,** (2011). Noise reduction of hyperspectral images using kernel non-negative tucker decomposition. *IEEE Journal of Selected Topics in Signal Processing*, 5(3), pp.487-493.
- Kiely, A.B. and Klimesh, M.A.,** (2009). Exploiting calibration-induced artifacts in lossless compression of hyperspectral imagery. *IEEE Transactions on Geoscience and Remote Sensing*, 47(8), pp.2672-2678.
- Koh, K., Kim, S.J. and Boyd, S.,** (2007). An interior-point method for large-scale  $l_1$ -regularized logistic regression. *Journal of Machine learning research*, 8(Jul), pp.1519-1555.
- Lam, A., Sato, I. and Sato, Y.,** (2012), November. Denoising hyperspectral images using spectral domain statistics. In *Pattern Recognition (ICPR), 2012 21st International Conference on* (pp. 477-480). IEEE.
- Lee, C., Youn, S., Jeong, T., Lee, E. and Serra-Sagrìstà, J.,** (2015). Hybrid compression of hyperspectral images based on PCA with pre-encoding discriminant information. *IEEE Geoscience and Remote Sensing Letters*, 12(7), pp.1491-1495.
- Lee, H., Battle, A., Raina, R. and Ng, A.Y.,** (2007). Efficient sparse coding algorithms. *Advances in neural information processing systems*, 19, p.801.
- Lee, H.S., Younan, N.H. and King, R.L.,** (2002). Hyperspectral image cube compression combining JPEG-2000 and spectral decorrelation. In *Geoscience and Remote Sensing Symposium, 2002. IGARSS'02. 2002 IEEE International* (Vol. 6, pp. 3317-3319). IEEE.
- Lee, S., Lee, E., Choi, H. and Lee, C.,** (2005), July. Compression of hyperspectral images with 2- levels wavelet transform using adjacent information and SPIHT algorithm. In *Geoscience and Remote Sensing Symposium, 2005. IGARSS'05. Proceedings. 2005 IEEE International* (Vol. 1, pp. 3-pp). IEEE.
- Li, S., Yin, H. and Fang, L.,** (2013). Remote sensing image fusion via sparse representations over learned dictionaries. *IEEE Transactions on Geoscience and Remote Sensing*, 51(9), pp.4779-4789.
- Li, W. and Du, Q.,** (2014). Joint within-class collaborative representation for hyperspectral image classification. *IEEE Journal of Selected Topics in Applied Earth Observations and Remote Sensing*, 7(6), pp.2200-2208.

- Licciardi, G.A., Chanussot, J. and Piscini, A.,** (2014), October. Spectral compression of hyperspectral images by means of nonlinear principal component analysis decorrelation. In *Image Processing (ICIP), 2014 IEEE International Conference on* (pp. 5092-5096). IEEE.
- Lin, T. and Bourennane, S.,** (2013). Hyperspectral image processing by jointly filtering wavelet component tensor. *IEEE Transactions on Geoscience and Remote Sensing*, 51(6), pp.3529-3541.
- Lu, T., Li, S., Fang, L., Ma, Y. and Benediktsson, J.A.,** (2016). Spectral-spatial adaptive sparse representation for hyperspectral image denoising. *IEEE Transactions on Geoscience and Remote Sensing*, 54(1), pp.373-385.
- Lu, X. and Su, L.,** (2016). Shrinkage estimation of dynamic panel data models with interactive fixed effects. *Journal of Econometrics*, 190(1), pp.148-175.
- Maggioni, M., Katkovnik, V., Egiazarian, K. and Foi, A.,** (2013). Nonlocal transform-domain filter for volumetric data denoising and reconstruction. *IEEE transactions on image processing*, 22(1), pp.119-133.
- Magli, E., Olmo, G. and Quacchio, E.,** (2004). Optimized onboard lossless and near-lossless compression of hyperspectral data using CALIC. *IEEE Geoscience and remote sensing letters*, 1(1), pp.21-25.
- Mairal, J., Bach, F., Ponce, J. and Sapiro, G.,** (2009), June. Online dictionary learning for sparse coding. In *Proceedings of the 26th annual international conference on machine learning* (pp. 689-696). ACM.
- Mairal, J., Bach, F., Ponce, J. and Sapiro, G.,** (2010). Online learning for matrix factorization and sparse coding. *Journal of Machine Learning Research*, 11(Jan), pp.19-60.
- Mairal, J., Elad, M. and Sapiro, G.,** (2008). Sparse representation for color image restoration. *IEEE Transactions on image processing*, 17(1), pp.53-69.
- Mairal, J., Elad, M. and Sapiro, G.,** (2008). Sparse representation for color image restoration. *IEEE Transactions on image processing*, 17(1), pp.53-69.
- Mallat, S.G. and Zhang, Z.,** (1993). Matching pursuits with time-frequency dictionaries. *IEEE Transactions on signal processing*, 41(12), pp.3397-3415.
- Mamatha, A.S. and Singh, V.,** (2014), September. Lossless hyperspectral image compression using intraband and interband predictors. In *Advances in Computing, Communications and Informatics (ICACCI), 2014 International Conference on* (pp. 332-337). IEEE.
- Memon, N.D., Sayood, K. and Magliveras, S.S.,** (1994). Lossless compression of multispectral image data. *IEEE Transactions on Geoscience and Remote Sensing*, 32(2), pp.282-289.
- Mielikainen, J. and Toivanen, P.,** (2003). Clustered DPCM for the lossless compression of hyperspectral images. *IEEE Transactions on Geoscience and Remote Sensing*, 41(12), pp.2943-2946.
- Nallathai, P., Jeyakumar, S. and Nithiyandam, N.,** (2013), December. Hyper spectral image compression based on non-iterative matrix factorization. In *Computational Intelligence and Computing Research (ICCIC), 2013 IEEE International Conference on* (pp. 1-4). IEEE.
- Ngadiran, R., Boussakta, S., Bouridane, A. and Syarif, B.,** (2010), July. Hyperspectral image compression with modified 3D SPECK. In *Communication Systems Networks and Digital Signal Processing (CSNDSP), 2010 7th International Symposium on* (pp. 806-810). IEEE.

- Othman, H. and Qian, S.E.**, (2006). Noise reduction of hyperspectral imagery using hybrid spatial-spectral derivative-domain wavelet shrinkage. *IEEE Transactions on Geoscience and Remote Sensing*, 44(2), pp.397-408.
- Peng, Y., Meng, D., Xu, Z., Gao, C., Yang, Y. and Zhang, B.**, (2014). Decomposable nonlocal tensor dictionary learning for multispectral image denoising. In *Proceedings of the IEEE Conference on Computer Vision and Pattern Recognition* (pp. 2949-2956).
- Penna, B., Tillo, T., Magli, E. and Olmo, G.**, (2005), July. Embedded lossy to lossless compression of hyperspectral images using JPEG 2000. In *Geoscience and Remote Sensing Symposium, 2005. IGARSS'05. Proceedings. 2005 IEEE International* (Vol. 1, pp. 4-pp). IEEE.
- Penna, B., Tillo, T., Magli, E. and Olmo, G.**, (2006). Progressive 3- levels coding of hyperspectral images based on JPEG 2000. *IEEE Geoscience and remote sensing letters*, 3(1), pp.125-129.
- Penna, B., Tillo, T., Magli, E. and Olmo, G.**, (2006). Progressive 3- levels coding of hyperspectral images based on JPEG 2000. *IEEE Geoscience and remote sensing letters*, 3(1), pp.125-129.
- Prasad, L. and Iyengar, S.S.**, (1997). *Wavelet analysis with applications to image processing*. CRC press.
- Prasad, S., Bruce, L. and Chanussot, J.**, (2011). *Optical remote sensing. Advances in Signal Processing and Exploitation Techniques*.
- Puri, A., Sharifahmadian, E. and Latifi, S.**, 2014. A Comparison of Hyperspectral Image Compression Methods. *International Journal of Computer and Electrical Engineering*, 6(6), p.493.
- Qian, Y. and Ye, M.**, (2013). Hyperspectral imagery restoration using nonlocal spectral-spatial structured sparse representation with noise estimation. *IEEE Journal of Selected Topics in Applied Earth Observations and Remote Sensing*, 6(2), pp.499-515.
- Qian, Y., Shen, Y., Ye, M. and Wang, Q.**, (2012), July. 3- levels nonlocal means filter with noise estimation for hyperspectral imagery denoising. In *Geoscience and Remote Sensing Symposium (IGARSS), 2012 IEEE International* (pp. 1345-1348). IEEE.
- Ramakrishna, B., Plaza, A.J., Chang, C.I., Ren, H., Du, Q. and Chang, C.C.**, (2006). Spectral/spatial hyperspectral image compression. In *Hyperspectral data compression* (pp. 309-346). Springer US.
- Ramakrishna, B., Wang, J., Chang, C.I., Plaza, A., Ren, H., Chang, C.C., Jensen, J.L. and Jensen, J.O.**, (2005), June. Spectral/spatial hyperspectral image compression in conjunction with virtual dimensionality. In *Defense and Security* (pp. 772-781). International Society for Optics and Photonics.
- Roger, R.E. and Cavenor, M.C.**, (1996). Lossless compression of AVIRIS images. *IEEE Transactions on Image Processing*, 5(5), pp.713-719.
- Romines, K.**, (2006). *Hyperspectral Image Compression with Optimization for Spectral Analysis* (Doctoral dissertation, University of Washington).
- Schelkens, P., Barbarien, J. and Cornelis, J.P.**, (2000), December. Compression of volumetric medical data based on cube splitting. In *International Symposium on Optical Science and Technology* (pp. 91-101). International Society for Optics and Photonics.



- Shahriyar, S., Paul, M., Murshed, M. and Ali, M.,** (2016), November. Lossless Hyperspectral Image Compression Using Binary Tree Based Decomposition. In *Digital Image Computing: Techniques and Applications (DICTA)*, 2016 International Conference on (pp. 1-8). IEEE.
- Şımşek, M. and Polat, E.,** (2015), October. The effect of dictionary learning algorithms on super-resolution hyperspectral reconstruction. In *Information, Communication and Automation Technologies (ICAT)*, 2015 XXV International Conference on (pp. 1-5). IEEE.
- Skretting, K. and Engan, K.,** (2011), May. Image compression using learned dictionaries by RLS-DLA and compared with K-SVD. In *Acoustics, Speech and Signal Processing (ICASSP)*, 2011 IEEE International Conference on (pp. 1517-1520). IEEE.
- Strang, G. and Nguyen, T.,** (1996). *Wavelets and filter banks*. SIAM.
- Tamhankar, H. and Fowler, J.E.,** (2007), July. Spectral-decorrelation strategies for the compression of hyperspectral imagery. In *Geoscience and Remote Sensing Symposium, 2007. IGARSS 2007. IEEE International* (pp. 1041-1044). IEEE.
- Tang, C., Cheung, N.M., Ortega, A. and Raghavendra, C.S.,** (2005), March. Efficient inter-band prediction and wavelet based compression for hyperspectral imagery: a distributed source coding approach. In *Data Compression Conference, 2005. Proceedings. DCC 2005* (pp. 437-446). IEEE.
- Tang, G. and Nehorai, A.,** (2010). Performance analysis for sparse support recovery. *IEEE transactions on information theory*, 56(3), pp.1383-1399.
- Tang, X. and Pearlman, W.A.,** (2006). Three-dimensional wavelet-based compression of hyperspectral images. In *Hyperspectral Data Compression* (pp. 273-308). Springer US.
- Tang, X., Pearlman, W.A. and Modestino, J.W.,** (2003), May. Hyperspectral image compression using three-dimensional wavelet coding. In *Proceedings of SPIE* (Vol. 5022, pp. 1037-1047).
- Tibshirani, R.,** (1996). Regression shrinkage and selection via the lasso. *Journal of the Royal Statistical Society. Series B (Methodological)*, pp.267-288.
- Töreym, B.U., Yilmaz, O., Mert, Y.M. and Türk, F.,** (2015), June. Lossless hyperspectral image compression using wavelet transform based spectral decorrelation. In *Recent Advances in Space Technologies (RAST)*, 2015 7th International Conference on (pp. 251-254). IEEE.
- Tropp, J.A.,** (2006). Algorithms for simultaneous sparse approximation. Part II: Convex relaxation. *Signal Processing*, 86(3), pp.589-602.
- Tropp, J.A., Gilbert, A.C. and Strauss, M.J.,** (2006). Algorithms for simultaneous sparse approximation. Part I: Greedy pursuit. *Signal Processing*, 86(3), pp.572-588.
- Ülkü, İ. and Töreym, B.U.,** (2014), November. Lossy compression of hyperspectral images using online learning based sparse coding. In *Computational Intelligence for Multimedia Understanding (IWCIM)*, 2014 International Workshop on (pp. 1-5). IEEE.
- Ülkü, İ. and Töreym, B.U.,** (2015a). Sparse coding of hyperspectral imagery using online learning. *Signal, Image and Video Processing*, 9(4), pp.959-966.
- Ülkü, İ. and Töreym, B.U.,** (2015b). Sparse representations for online-learning-based hyperspectral image compression. *Applied Optics*, 54(29), pp.8625-8631.

- Ülkü, İ. and Töreyn, B.U.**, (2015c), May. Hyperspectral image compression using an online learning method. In SPIE Sensing Technology+ Applications (pp. 950104-950104). International Society for Optics and Photonics.
- Url-1**< [http://www.hyspex.no/hyperspectral\\_imaging/](http://www.hyspex.no/hyperspectral_imaging/) >, date retrieved 05.04.2017.
- Wang, C., Jiao, A. and Li, J.**, (1998), August. Transform coding compression of hyperspectral image. In Asia-Pacific Symposium on Remote Sensing of the Atmosphere, Environment, and Space (pp. 69-78). International Society for Optics and Photonics.
- Wang, H. and Celik, T.**, (2016), July. Sparse representation based lossy hyperspectral data compression. In Geoscience and Remote Sensing Symposium (IGARSS), 2016 IEEE International (pp. 2761-2764). IEEE.
- Wang, H., Babacan, S.D. and Sayood, K.**, (2007). Lossless hyperspectral-image compression using context-based conditional average. *IEEE transactions on geoscience and remote sensing*, 45(12), pp.4187-4193.
- Wang, J., Zhang, M. and Tang, S.**, (1995). Spectral and spatial decorrelation of Landsat-TM data for lossless compression. *IEEE Transactions on Geoscience and Remote Sensing*, 33(5), pp.1277-1285.
- Wang, L., Wu, H. and Pan, C.**, (2015). Manifold regularized local sparse representation for face recognition. *IEEE Transactions on Circuits and Systems for Video Technology*, 25(4), pp.651-659.
- Wang, L., Wu, J., Jiao, L. and Shi, G.**, (2009). Lossy-to-lossless hyperspectral image compression based on multiplierless reversible integer TDLT/KLT. *IEEE Geoscience and remote sensing letters*, 6(3), pp.587-591.
- Wang, Y. and Niu, R.**, (2009), May. Hyperspectral urban remote sensing image smoothing and enhancement using forward-and-backward diffusion. In Urban Remote Sensing Event, 2009 Joint (pp. 1-5). IEEE.
- Wang, Y., Niu, R. and Yu, X.**, (2010). Anisotropic diffusion for hyperspectral imagery enhancement. *IEEE Sensors Journal*, 10(3), pp.469-477.
- Wang, Z., Nasrabadi, N.M. and Huang, T.S.**, (2014). Spatial-spectral classification of hyperspectral images using discriminative dictionary designed by learning vector quantization. *IEEE Transactions on Geoscience and Remote Sensing*, 52(8), pp.4808-4822.
- Willett, R.M., Duarte, M.F., Davenport, M.A. and Baraniuk, R.G.**, (2014). Sparsity and structure in hyperspectral imaging: Sensing, reconstruction, and target detection. *IEEE signal processing magazine*, 31(1), pp.116-126.
- Wu, X. and Memon, N.**, (2000). Context-based lossless interband compression-extending CALIC. *IEEE Transactions on Image Processing*, 9(6), pp.994-1001.
- Xie, Y., Ho, J. and Vemuri, B.**, (2013). On a nonlinear generalization of sparse coding and dictionary learning. In Proceedings of the 30th International Conference on Machine Learning, NIH Public Access (p. 1480).
- Yang, J., Peng, Y., Xu, W. and Dai, Q.**, (2009). Ways to sparse representation: an overview. *Science in China series F: information sciences*, 52(4), pp.695-703.
- Yang, J., Wright, J., Huang, T.S. and Ma, Y.**, (2010). Image super-resolution via sparse representation. *IEEE transactions on image processing*, 19(11), pp.2861-2873.
- Yang, J., Xu, W., Dai, Q. and Wang, Y.**, (2007), May. Image compression using 2-levels Dual-tree discrete wavelet transform (DDWT). In Circuits and Systems, 2007. ISCAS 2007. IEEE International Symposium on (pp. 297-300). IEEE.

- Yang, Y., Liu, B., Duan, X. and Nian, Y.,** (2014), October. Hyperspectral images compression based on independent component analysis: ROI-based compression algorithm for hyperspectral images. In *Image and Signal Processing (CISP), 2014 7th International Congress on* (pp. 771-777). IEEE.
- Yuan, Q., Zhang, L. and Shen, H.,** (2012). Hyperspectral image denoising employing a spectral–spatial adaptive total variation model. *IEEE Transactions on Geoscience and Remote Sensing*, 50(10), pp.3660-3677.
- Zhang, H., He, W., Zhang, L., Shen, H. and Yuan, Q.,** (2014). Hyperspectral image restoration using low-rank matrix recovery. *IEEE Transactions on Geoscience and Remote Sensing*, 52(8), pp.4729-4743.
- Zhang, L., Zhang, Q., Zhang, L., Tao, D., Huang, X. and Du, B.,** (2015). Ensemble manifold regularized sparse low-rank approximation for multiview feature embedding. *Pattern Recognition*, 48(10), pp.3102-3112.
- Zhang, Y., Liu, J., Yang, W. and Guo, Z.,** (2015). Image super-resolution based on structure-modulated sparse representation. *IEEE Transactions on Image Processing*, 24(9), pp.2797-2810.
- Zhang, Z., Xu, Y., Yang, J., Li, X. and Zhang, D.,** (2015). A survey of sparse representation: algorithms and applications. *IEEE access*, 3, pp.490-530.
- Zhong, P. and Wang, R.,** (2013). Multiple-spectral-band CRFs for denoising junk bands of hyperspectral imagery. *IEEE Transactions on Geoscience and Remote Sensing*, 51(4), pp.2260-2275.
- Zhou, Z., Liu, J. and Tian, J.,** (2006), November. Real-time hyperspectral image cube compression combining adaptive classification and partial transform coding. In *Signal Processing, 2006 8th International Conference on* (Vol. 2). IEEE.



## CURRICULUM VITAE

**Name Surname:** Hayder Abdulsattar Nahi Jawdhari

**Place and date of birth:** IRAQ\BABIL, 18\12\1989

**Address:** IRAQ \ BABIL \ AI-QASSIM CITY.

**E-Mail:** [jawdhari15@itu.edu.tr](mailto:jawdhari15@itu.edu.tr), [haidersatar189@yahoo.com](mailto:haidersatar189@yahoo.com)

**B.Sc.:** 2011, Al-Qadisiyah University, College of Science, Computer Science

**Professional Experience and Rewards:** Research assistant at Al\_Qassim Green University, Director of the university's website

